On the stability and control of piecewise-smooth dynamical systems with impacts and friction

Fredrik Svahn

Doctoral Thesis

TRITA-AVE 2009:66
ISSN 1651-7660
ISBN 978-91-7415-437-5

Postal address	**Visiting address**	**Telephone**	**Internet**
Royal Institute of Technology	Teknikringen 8	+46 8 790 6000	www.ave.kth.se
Vehicle Dynamics	Stockholm	**Telefax**	
SE-100 44 Stockholm		+46 8 790 9290	

Typset in LaTeX

Abstract

This thesis concerns the analysis of dynamical systems suitable to be modelled by piecewise-smooth differential equations. In such systems the continuous-in-time dynamics is interrupted by discrete-in-time jumps in the state or governing equations of motion. Not only can this framework be used to describe existing systems with strong nonlinear behaviour such as impacts and friction, but the non-smooth properties can be exploited to design new mechanical devices. As suggested in this work it opens up the possibility of, for example, fast limit switches and energy transfer mechanisms.

Particularly, the dynamics at the onset of low-velocity impacts in systems with recurrent dynamics, so called *grazing bifurcations* in impact-oscillators, are investigated. As previous work has shown, low-velocity impacts is a strong source of instability to the dynamics, and efforts to control the behaviour is of importance. This problem is approached in two ways in this work. One is to investigate the influence of parameter variations on the dynamic behaviour of the system. The other is to implement low-cost control strategies to regulate the dynamics at the grazing bifurcation. The control inputs are of impulsive nature, and utilizes the natural dynamics of the system to the greatest extent.

The scientific contributions of this work is collected in five appended papers. The first paper consists of an experimental verification of a map that captures the correction to the smooth dynamics induced by an impact, known in the literature as the *discontinuity map*. It is shown that the lowest order expansion of the map accurately captures the transient growth rate of impact velocities. The second paper presents a constructive proof of a control algorithm for a rather large class of impact oscillators. The proof is constructive in the sense that it gives control parameters which stabilizes the dynamics at the onset of low-velocity impacts. In the third paper a piecewise-smooth quarter-car model is derived, and the control strategy is implemented to reduce impact velocities in the suspension system. In the fourth and fifth papers the grazing bifurcation of an impact oscillator with dry friction type damping is investigated. It turns out that the bifurcation is triggered by the disappearance of an interval of stable stick solutions. A condition on the parameters of the system is derived which differentiates between stable and unstable types of bifurcation scenarios. Additionally, a low-cost control strategy is proposed, similar to the one previously mentioned, to regulate the bifurcation scenario.

Preface

Warum etwas einfach machen wenn man es so schön komplizieren kann?[1]

These words have occasionally run through my head during the work for this thesis. Yes, why make something so beautifully complicated when on the face of it, it seems so simple? Like bouncing a ball on a tennis racket. Sure, it takes some practice but it is still just two objects occasionally colliding. However, thinking about the physics behind the motion and attempting to describe it in mathematical terms suddenly makes it very complicated. How do I describe the forces involved in the impact between the ball and the racket? What adjustments does the arm have to do to keep the ball in a steady bounce? The math involved in finding those formulas is frustratingly complicated. But when it works, it sure is beautiful.

Acknowledgement

This research project has been performed at KTH Vehicle Dynamics, Royal Institute of Technology, Stockholm, Sweden, in collaboration with the Department of Mechanical Science and Engineering at University of Illinois at Urbana-Champaign, USA. I am truly grateful for the financial support of the Swedish Research Council (Vetenskapsrådet), and in the extension the Swedish taxpayers, for making this project possible.

First of all I would like to thank my co-advisor Professor Annika Stensson Trigell for initiating the project, providing me with feedback on my work and keeping me on track in the project.

Also, I am very much indebted to my co-advisor and closest collaborator Professor Harry Dankowicz at UIUC for putting so much energy into the project and giving me so much of his time, patiently explaining and answering questions about the intricate subject of non-smooth dynamics. It has been a pleasure to work with you, and to take part of your knowledge and never ending enthusiasm. I am also grateful to you for three very rewarding and fun research stays at

[1] German saying which translates into "Why make something easy when you can make it so beatifully complicated?"

UIUC. The guys at the Applied Dynamics Lab, especially Phani and Bryan; you very much contributed to the enjoyment of my visits.

My third co-advisor, Assistant Professor Jenny Jerrelind; thanks for all the guidance and encouragement, it is a pleasure to work with you.

Thanks to Bryan Wilcox for a great collaboration, for proof reading this thesis and for all the serious and non-serious discussions we have had. A special thanks to Petri Piiroinen who invited me to an interesting and valuable one week stay of research at the National University of Ireland in Galway. I am glad we also had time for some intake of fine Irish brews together.

To all my colleagues at KTH Vehicle Dynamics; thanks to you it has been a pleasure to come to work every day, its great to enjoy a cup of coffee with you or chat over a pint after work. A thought also goes to all the other interesting people I have come across during the course of these years, at the department, at KTH-hallen (there is nothing like exercise to clear the head!) and during all my work-related trips. Had I not pursued this project I would have missed all those enriching meetings.

Thanks to my family and relatives for letting me use the summer cottages for three productive stays of half-seclution and especially to my sister and her family for providing me with some human contact and nourishment during the evenings. Also, very much thank you to my relatives in Illinois who have taken care of me during several visits, especially Kerry, Louis and Walter (who I am lucky to have had the opportunity to spend time with before he passed away). Your hospitality is astounding and I feel like I have a second home on the other side of the globe.

Last but not least to my parents, my brother and his family and again to my sister and her family; you have supported and encouraged me all along even though you are not always sure of what I do. I am so glad to have you all!

Fredrik Svahn
Stockholm, Sweden, September 2009

Appended papers

Paper A

B. Wilcox, F. Svahn, H. Dankowicz, J. Jerrelind, Transient growth rates of near-grazing impact velocities: theory and experiments, *Journal of Sound and Vibration*, **325(4-5)**, pp. 950-958, 2009. (doi:10.1016/j.jsv.2009.04.012)

Paper B

H. Dankowicz and F. Svahn, On the stabilizability of near-grazing dynamics in impact oscillators, *International journal of robust and nonlinear control*, **17(15),** pp. 1405-1429, 2007. (doi:10.1002/rnc.1252)

Paper C

F. Svahn, J. Jerrelind and H. Dankowicz, Suppression of bumpstop instabilities in a quarter-car model. In *Non-smooth Problems in Vehicle Systems Dynamics - Proceedings of the Euromech Colloquium* (eds. P. Grove Thomsen and H. True), Springer Verlag, ISBN 978-3-642-01355-3, 2009. (doi:10.1007/978-3-642-01356-0_12)

Paper D

F. Svahn and H. Dankowicz, Energy transfer in vibratory systems with friction exhibiting low-velocity collisions, *Journal of vibration and control*, **14**, pp. 255-284, 2008. (doi:10.1177/1077546307079390)

Paper E

F. Svahn and H. Dankowicz, Controlled onset of low-velocity collisions in a vibro-impacting system with friction, to appear in *Proceedings of the Royal So-*

ciety A: Mathematical, Physical and Engineering Sciences, 2009. (doi:10.1098/rspa.2009.0207)

Contributions of individual authors

Paper A: Fredrik Svahn and Bryan Wilcox planned, performed and analysed the experiments jointly, with feedback from Professor Harry Dankowicz and Assistant Professor Jenny Jerrelind. Fredrik Svahn and Harry Dankowicz performed the analysis and the simulations were done by Bryan Wilcox. The paper was written jointly by the authors.

Paper B: Professor Harry Dankowicz performed analysis, simulations and derivation of the control algorithm. Fredrik Svahn performed analysis and simulations. Paper predominantly written by Professor Harry Dankowicz.

Paper C: Fredrik Svahn did modelling, analysis, simulations and co-wrote the paper with Professor Harry Dankowicz. Harry Dankowicz and Assistant Professor Jenny Jerrelind provided feedback throughout the work.

Paper D: Analysis predominantly by Fredrik Svahn, simulations and writing by both authors.

Paper E: Analysis was done in equal parts by the two authors, simulations by Fredrik Svahn. The paper was co-written by the two authors.

Contents

Chapter 1

Introduction

1.1 Background

The human urge to understand and describe motion has a long history. As always, the ancient Greeks were the first to delve into the subject seriously and the laws of motion that the philosopher Aristotle formulated was generally accepted as the truth for almost 2000 years. He was not firmly superseded until Isaac Newton published his seminal work *Principia* in 1687 including his famous three laws of motion. Meanwhile, Newton and Gottfried Leibniz independently developed differential and integral calculus which is the basis for the mathematical description of motion [1]. Thus, the field of mathematical modelling of dynamical systems was opened up and has since generated an explosion of scientific work. These mathematical models can be used to understand and predict the dynamic behaviour of physical systems. Most commonly, linear dynamical equations are used as they are easy to analyse, an approach which has no doubt proven to be very fruitful. However, some physical systems are very poorly described by linear equations and in those cases nonlinear descriptions have to be employed. Of particular interest in this thesis are systems where some parts of the dynamics lives on a different time scale than the rest. Such phenomenon include impacts where contact forces suddenly and rapidly increase with an associated rapid change in velocity of the impacting object. Another example is a dry friction force which instantly switches from positive to negative as the velocity of the exposed object transitions through zero. Such dynamical systems has to be modelled with nonlinear equations and a particularly suitable way, pursued in this work, is to model them with discrete jumps in the equations describing the dynamics. This type of nonlinear dynamical systems are usually called *piecewise-smooth* or *non-smooth* dynamical systems. The terms are used interchangeably in this thesis.

The topic of this work is systems with recurrent dynamics and impacts, so called *impact oscillators*, and particularly the onset of low-velocity impacts in such systems. Physical systems where impacts can occur are numerous;

train current collector suspensions [2], impact microactuators [3–5], gears [6], clearance in ball bearings [7], Braille printers [8,9], car suspensions [10], granular flow [11], among others. See also [12] for a survey of nonlinearities, including impacts, in engineering systems.

Impacting systems, and particularly low-velocity, or *grazing*, impacts, have been extensively studied through the years. Shaw and co-workers made considerable contributions to this area in the 1980's. They noted that a zero velocity impact gives a singularity in the equations describing the dynamics [13]. See also [14, 15] for further studies of impacting dynamics. Following their work, Nordmark derived a map, referred to as the *discontinuity map*, describing the correction to the non-impacting dynamics induced by the grazing bifurcation [16]. He found that the discontinuity map contains a square root term implying that the derivative of the map is singular at the point of grazing contact. Conditions for the nature of the near-grazing dynamics were also derived. Attractors with near-grazing dynamics of different kinds of impact oscillators were explored in [17]. Chin, Ott et al. further analysed the map regarding the different kinds of bifurcations which are possible in a one-degree-of-freedom impact oscillator [18]. In [19–21] the theory of the discontinuity mapping is further developed for more complex systems and [22] contains an experimental verification of the discontinuity map. See also [23–25] for other experiments on grazing impacts. Previous work on impact oscillators with friction, which this thesis is partly about, is limited but some references are [26–29].

The focus of this work is the stability properties of the dynamics at the onset of low-velocity impacts in a selection of different impact-oscillators. The basic idea is to investigate how the parameters of the system determines the dynamics after the onset of impacts. Such investigations are important when designing engineering systems to optimize performance. If the desirable dynamics is impossible to attain with realistic parameters, a natural step is to implement a control system to enhance the performance. To this end, this work proposes control strategies that rely on discrete inputs to the system to utilize the natural dynamics as much as possible, and thereby minimize the energy consumption of the control.

1.2 Objective

The overall objective of the research project is to investigate to what extent properties and analysis techniques of non-smooth dynamical systems can be exploited to improve present engineering systems, or for design of completely new ones not realizable with linear dynamics. For example, the impact-oscillators considered could be the basis for design of devices for transmission of energy between different parts of a system, or the construction of limit switches triggered by the onset of impacts. Additionally, it is investigated to what extent a car suspension system could be improved by controlling low-velocity impacts.

Particularly, the aim of this work is to continue previous efforts *to determine the nature of the dynamics at the onset of low-velocity impacts in piecewise-smooth systems and develop low-cost control strategies to regulate such dynamics.*

1.3 Outline of thesis

The scientific contributions of this work are collected in **Papers A-E,** appended at the end of the thesis. In addition, there is a main body which includes a summary of the research performed and explanations of methods and theoretical tools used in the appended papers.

Chapter 2 gives an introduction to nonlinear dynamical systems, with emphasis on piecewise-smooth systems, and the theoretical tools available to analyse them. Chapter 3 gives a brief description of the mechanical models considered in the appended papers. Chapter 4 gives an overview of control of piecewise-smooth systems. Chapter 5 contains a summary of the appended papers, one section on the control methods proposed in this thesis, and two shorter sections with additional material to **Paper E**. Finally, Chapters 6 and 7 contains a general discussion of the results along with some conclusions and ideas for future work. The nomenclature can be found after the references in the main body.

Chapter 2

Nonlinear dynamics

This chapter aims to give the reader an overview of the theoretical tools and concepts used in the appended papers. The literature on nonlinear dynamics is vast. See for example [30] for smooth nonlinear systems and [31] for non-smooth dynamical systems. The chapter is outlined as follows. First, the concept of dynamical systems is introduced, after which we turn attention to the special class of dynamical systems which are piecewise-smooth. A short section on transient versus steady-state dynamics is followed by the important topic of stability of dynamical systems. The phenomenon of chaotic dynamics is then described, before a section on the other core topic of this work; bifurcations, which concerns qualitative changes in the dynamics as a parameter of the system is varied. The chapter concludes with a brief description of the numerical tools used in the appended papers.

2.1 Dynamical systems

The mathematical formalism of differential equations has proven useful for describing dynamical systems, that is the evolution of a system with respect to an independent variable, usually time. There are two main types of differential equations; ordinary- and partial differential equations. Ordinary differential equations only include derivatives with respect to one independent variable, whereas partial differential equations include derivatives with respect to more than one variable. In this thesis only ordinary differential equations, with time as the independent variable, are considered. All ordinary differential equations can be written as a system of first order derivatives, the *state space form*:

$$\dot{\mathbf{x}} = \mathbf{f}(\mathbf{x}), \mathbf{x} \in \mathbb{R}^n, \tag{2.1}$$

where $\mathbf{x}$ is a vector of all the states of the system, $\mathbf{f}$ is some function, $(\dot{})$ denotes differentiation with respect to time and n is called the *dimension* of the system. The right hand side of this equality is referred to as the *vector field*, since to

each point $\mathbf{x}$ a vector $\mathbf{f}(\mathbf{x})$ is associated which points in the direction of the solution. Equation 2.1 together with an initial state

$$\mathbf{x}(t_0) = \mathbf{x}_0 \tag{2.2}$$

defines a solution to the system.

If $\mathbf{f}(\mathbf{x})$ is a linear function in $\mathbf{x}$, then the system in Equation 2.1 is said to be a *linear system*. In all other cases it is a *nonlinear system*.

The vector field in Equation 2.1 is not explicitly dependent on time which makes it an *autonomous* dynamical system. This assumption can however be made without loss of generality since *non-autonomous* dynamical systems, with a vector field $\mathbf{f}(\mathbf{x},t)$, can be transformed to autonomous form by introducing time as an additional state variable. This thesis concerns periodically forced systems and typically a new state $\theta = \omega t$ is introduced which makes $\mathbf{f}$ have ω as its last component. The additional state θ is usually denoted the phase of the system.

A nonlinear initial value problem of the form presented in Equations 2.1-2.2 rarely admits an explicit solution. For analytical purposes, let $\mathbf{\Phi}(\mathbf{x},t)$, the *flow*, represent the state of the system after a time t of flowing along the trajectory which starts at the point $\mathbf{x}$. The initial value problem can then be expressed in terms of the flow as

$$\begin{matrix} \mathbf{\Phi}_{,t}(\mathbf{x},t) = \mathbf{f}(\mathbf{\Phi}(\mathbf{x},t)) \\ \mathbf{\Phi}(\mathbf{x},0) = \mathbf{x} \end{matrix} , \tag{2.3}$$

for all $\mathbf{x}$ and t.

Another way to model dynamical systems is to use *maps* in which time is discrete, not continuous as in differential equations. A map is defined as

$$\mathbf{x} \mapsto \mathbf{P}(\mathbf{x}), \ \mathbf{x} \in \mathbb{R}^n \tag{2.4}$$

where $\mathbf{P}$ is some function. Maps can be used to model natural phenomena such as impacts. They can also be used to describe and analyse solutions of differential equations, a method which is used in **Paper D**.

2.2 Piecewise-smooth dynamical systems

Piecewise-smooth dynamical systems are defined as dynamical systems with continuous-in-time dynamics interrupted by discrete-in-time changes in state and/or vector field at well defined boundaries in state space. Essentially, if the description of the system requires additional conditions apart from Equation 2.1 then it is a piecewise-smooth system. Such changes in the dynamics occur at *discontinuity surfaces* in state space, usually defined as the zero-level sets of smooth *event functions*. In this thesis these functions are denoted by h. A system with discontinuities is always defined as nonlinear.

A typical example of a jump in state is a jump in velocity associated with a non-compliant impact. Examples of systems with piecewisely defined governing

equations are dynamical systems with dry friction. Furthermore, many nonlinear electrical circuit elements can be approximately described as non-smooth, e.g. diodes and transistors. Discontinuities can also be enforced on systems through control. Especially in implementation of optimal control the input is often switched between extreme values (also known as bang-bang control). Essentially, any systems where some feature of the system occurs on a time scale much faster than the regular dynamics can be approximated by a piecewise-smooth system. Dynamical systems governed by both smooth flows and maps are sometimes referred to as *hybrid dynamical systems*. The term is commonly used in the field of systems and control [32].

There are different classes of piecewise-smooth systems and one way to categorize them is:

1. Non-smooth continuous systems, meaning the vector field is continuous but is non-differentiable at some order. One example is the car suspension in **Paper C** in this thesis modelled with piecewise linear damping.

2. Systems with discrete jumps in the vector field. One example is systems with dry friction as in **Papers D** and **E**. These systems are also known as *Filippov-systems* [33].

3. Systems with discrete jumps in state. Examples are systems with impacts where the velocity switches direction instantaneously at some discontinuity surface in state space. See **Papers A** to **E** for examples.

Inspiration for this categorization comes from [33]. In [31] this categorization is formalized into what is called *degree-of-smoothness*. Category 1 above then has a degree-of-smoothness two or higher (depending on which order of the vector field is non-differentiable), category 2 a degree-of-smoothness one and category 3 a degree-of-smoothness zero.

2.2.1 Impacts

Impact implies a sudden and brief rise in forces exerted on a body colliding with another object and is a strong nonlinearity when viewed from a dynamical systems perspective. It is therefore natural to model impacts in the piecewise-smooth framework. For impacts where the duration of contact is relatively long, a compliant impact model is appropriate. This is typically modelled as contact with a stiff spring and a damper. On the other hand, if the time duration of the impact is relatively short, an instantaneous jump in velocity according to Newtons impact law

$$v_{rel}|_{after} = -e\, v_{rel}|_{before}\,, \tag{2.5}$$

where e is called the *coefficient of restitution* and v_{rel} is the relative velocity of the colliding bodies, is usually sufficient. $e \in [0, 1]$ is a measure of the amount of kinetic energy dissipated in the collision. For further discussions of modelling impacts see [34]. Equation 2.5 together with the law of conservation

of momentum defines the state of the system after the impact. In this thesis the latter non-compliant impact law is used throughout.

The onset of low-velocity impacts in a periodic orbit can be severely destabilizing to the dynamics. See, for example, Section 2.6.2 for how the dynamical influence of low-velocity impacts and the associated bifurcation can be analysed.

2.2.2 Friction

An object in contact with a surface with an applied force tangential to the surface will be exposed to a force called *friction*. In the case of *dry friction* this force can counteract a certain amount of applied force such that if the object is initially at rest it remains at rest. The resistive force is called the *static friction force* and the object is said to be in a *stick* phase. However, if the applied force is larger than the maximum static friction the object starts to move relative to the surface. The object is then said to be in a *sliding* phase. The friction force in the sliding phase is called the *dynamic friction force* and is a function of the relative velocity. Typically, the maximum value of the static friction is larger than the dynamic friction.

There are many ways of modelling friction mathematically as it is a complex phenomenon [33]. Figure 2.1 shows three of the most common ones. Panel (a) shows the friction modelled by a smooth function. The flaw of this model is that it has no static friction; as soon as a force is applied, the two bodies will start to slide. Also, the steep slope around zero relative velocity compared to the slope for large relative velocities makes the problem difficult to solve from a numerical perspective (known as a *stiff* numerical problem). Panel (b) shows a non-smooth model of the friction which accurately captures the stick properties of the friction as well as the lower dynamic friction compared to the maximum static friction. This model can account for stick-slip instabilities for a mass in contact with a moving belt, see [33, 54]. Panel (c) shows a simple piecewise smooth friction model which captures the stick phenomenon with defined static and dynamic friction coefficients. In **Paper A** the Coulomb-Amonton model is used which is defined as in Figure 2.1(c) but with $F_s = F_d$.

From a mathematical point of view, dry friction manifests itself as the vector field having a jump at the zero relative velocity of the two objects in contact, i.e.

$$\mathbf{f}(\mathbf{x}) = \begin{cases} \mathbf{f}_1(\mathbf{x}) & v_{rel} > 0 \\ \mathbf{f}_2(\mathbf{x}) & v_{rel} < 0 \end{cases}, \tag{2.6}$$

with $\mathbf{f}_1(\mathbf{x}) \neq \mathbf{f}_2(\mathbf{x})$ when $v_{rel} = 0$. A jump in the vector field at some discontinuity surface implies that the discontinuity surface can be attracting from both sides in certain subsets of state space. Trajectories are then bound to follow trajectories on the discontinuity surface, so called *sliding solutions*. For example, the vector field of the friction oscillator in absence of impacts in **Papers D** and **E** has an attracting region of equilibrium points which corresponds to a stationary object. The terminology might be confusing since a sliding solution here corresponds to a stationary object but this is not necessarily the case for

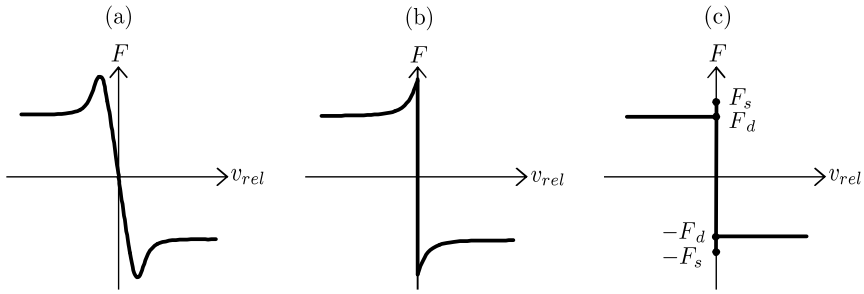

Figure 2.1: Different friction models. v_{rel} is the relative velocity of the two bodies and F is the friction force. (a) shows a smooth model of friction, (b) shows a non-smooth model with a smooth transition between static and dynamic friction and (c) shows a non-smooth model with F_s as a static friction coefficient and F_d as a dynamic friction coefficient.

general Filippov systems. Also, the equilibrium points can here be viewed as sliding along the phase-variable in state space.

The vector field for the sliding solutions can be calculated from Filippov's method by taking a convex combination of $\mathbf{f}_1$ and $\mathbf{f}_2$,

$$\mathbf{f}_{12} = (1-\alpha)\,\mathbf{f}_1 + \alpha \mathbf{f}_2, \tag{2.7}$$

with $0 \leq \alpha \leq 1$, where

$$\alpha\,(\mathbf{x}) = \frac{h_{,\mathbf{x}} \cdot \mathbf{f}_1}{h_{,\mathbf{x}} \cdot (\mathbf{f}_1 - \mathbf{f}_2)}, \tag{2.8}$$

and $h\,(\mathbf{x}) = 0$ defines the discontinuity surface [31]. For example, in **Papers D** and **E** the vector fields are $\mathbf{f}_1 = \begin{pmatrix} x_2 & -1-x_1 & \omega \end{pmatrix}^T$ and $\mathbf{f}_2 = \begin{pmatrix} x_2 & 1-x_1 & \omega \end{pmatrix}^T$ and $h\,(\mathbf{x}) = x_2$. Then $\alpha\,(\mathbf{x}) = (1+x_1)/2$ and thus the sliding vector field is $\mathbf{f}_{12} = \begin{pmatrix} 0 & 0 & \omega \end{pmatrix}^T$.

2.3 Transient and steady-state dynamics

There are two phases in the time evolution of a dynamical system. The initial dynamics is called the *transient response*. It is a product of the initial state of the system and eventually saturates. What remains is the *steady-state response* of the system, which in the linear case is independent of the initial value. On the other hand, for nonlinear systems multiple coexisting steady-state solutions are possible, and the initial state determines what solution is approached.

Investigations of the stability properties of a dynamical system usually regards the steady-state motion, and in that sense the steady-state motion is the

most important part of the dynamics. However, in engineering systems transients might be of equal importance and as the type of dynamics in transients is rich, including irregular chaos like motions, it often has to be investigated as well. One example is the operation of a Braille printer [9]. For some systems the operating time might even be shorter than the transient response in which case steady-state is never reached, for example an evasive manoeuvre of a road vehicle. **Paper A** particularly investigates the transient dynamics of an impact oscillator, whereas **Papers B** to **E** concerns the fate of the steady-state dynamics.

2.4 Stability

Stability issues of the steady-state dynamics is fundamental to dynamical system analysis. Tightly associated with the fate of the steady-state dynamics are the *invariant sets* of the system. An invariant set is a subset of state space with the property that any trajectory which reaches or starts in the set remains in the set for all future time. Invariant sets can either be repelling or attracting, in the latter case they are sometimes called *attractors*. In this thesis, fixed points of maps and periodic orbits are two types of invariant sets of particular importance. A special type of invariant set is the chaotic attractor described in Section 2.5.

2.4.1 Equilibrium points

Associated with the stability of dynamical systems are the *equilibrium points* defined when the vector field is equal to zero,

$$\mathbf{f}(\mathbf{x}) = 0. \tag{2.9}$$

By a change of coordinates all equilibrium points can be shifted to the origin, so without loss of generality, equilibrium points can be assumed to lie at the origin. The formal definition of local stability of an equilibrium point is then [35]:

Definition 1 *An equilibrium point, $\mathbf{x} = 0$, of an autonomous system, Equation 2.1, is* stable *if, for each $\epsilon > 0$, there exists a $\delta = \delta(\epsilon) > 0$ such that*

$$\|\mathbf{x}(0)\| < \delta \Rightarrow \|\mathbf{x}(t)\| < \epsilon, \ \forall\, t \geq 0. \tag{2.10}$$

The equilibrium point is unstable if it is not stable.

The equilibrium point is asymptotically stable if it is stable and δ can be chosen such that

$$\|\mathbf{x}(0)\| < \delta \Rightarrow \lim_{t\to\infty} \mathbf{x}(t) = 0.$$

For a stable equilibrium point the definition means that for any ϵ-size ball around the origin it must be possible to find a δ-size ball around the origin such that any trajectory starting therein remains in the ϵ-ball for all future time.

2.4.2 Periodic solutions

A focus of this thesis is local stability of periodic solutions. Stability of such solutions can be analysed in a similar manner as equilibrium points. Let $\mathbf{x}_p(t)$ be a periodic solution, i.e. $\mathbf{x}_p(t) = \mathbf{x}_p(t+T)$ for some constant T, of the system described by Equation 2.1, and define an ϵ-neighbourhood of $\mathbf{x}_p(t)$ as

$$U_\epsilon = \{\mathbf{x} \,|\, \inf \|\mathbf{x} - \mathbf{x}_p(t)\| < \epsilon\}, \tag{2.11}$$

where $\inf \|\mathbf{x} - \mathbf{x}_p(t)\|$ is the minimum distance from the point $\mathbf{x}$ to the periodic orbit $\mathbf{x}_p(t)$. The definition of local stability of $\mathbf{x}_p(t)$ is then [35]:

Definition 2 *The periodic solution $\mathbf{x}_p(t)$ of the system in Equation 2.1 is stable if, for each $\epsilon > 0$, there is a $\delta > 0$ such that*

$$\mathbf{x}(0) \in U_\delta \Rightarrow \mathbf{x}(t) \in U_\epsilon, \ \forall\, t \geq 0, \tag{2.12}$$

and asymptotically stable if it is stable and δ can be chosen such that

$$\mathbf{x}(0) \in U_\delta \Rightarrow \lim_{t\to\infty} \inf \|\mathbf{x}(t) - \mathbf{x}_p(t)\| = 0. \tag{2.13}$$

Isolated periodic solutions are often denoted *limit cycles*. If the period time, T, of the solution is compared to the period of the excitation, a classification of the response can be made. Let $T_f = \frac{2\pi}{\omega}$ be the period of the forcing, where ω is its angular frequency. If $T/T_f = 1$, i.e. if the response has the same period as the forcing the response is called *harmonic*. If $T/T_f = n$, $n = 2, 3, 4, \ldots$ the response is called *subharmonic* motion of order n, also called an *n-periodic* motion.

Periodic motion has a single fundamental frequency $1/T$. Also, there is a more complicated type of invariant set called *quasiperiodic motion*, which is motion with a finite number (two or more) of fundamental frequencies. Quasi-periodic solutions can be represented as motions on a torus in phase space (a doughnut-shaped set) on which the trajectories revolve endlessly without ever intersecting, [30, 36].

2.4.3 Stability of maps

Similarly to equilibrium points of differential equations, maps can have what is called fixed points. $\mathbf{x}^*$ is then a fixed point of the map if

$$\mathbf{P}(\mathbf{x}^*) = \mathbf{x}^*. \tag{2.14}$$

A fixed point of the n-th iterate of the map is called a period-n point.

Assume that the map, P, is a one-dimensional nonlinear map with a fixed point $x^* = P(x^*)$. Then small perturbations from the fixed point, ϵ, is linearly governed by the map

$$\epsilon \mapsto P_{,x}(x^*)\,\epsilon. \tag{2.15}$$

After k iterations of the map the result is $\left(P_{,x}\left(x^*\right)\right)^k \epsilon$. Hence, if $\left|P_{,x}\left(x^*\right)\right| < 1$ perturbations away from x^* eventually decays to zero and the fixed point is linearly stable. On the other hand, if $\left|P_{,x}\left(x^*\right)\right| > 1$ the fixed point is unstable, and if $\left|P_{,x}\left(x^*\right)\right| = 1$ a nonlinear analysis is necessary to determine stability. $P_{,x}\left(x^*\right)$ is here the eigenvalue, or *multiplier* of the map. Similarly, for higher dimensional maps all eigenvalues of the Jacobian of the map has to have an absolute value less than one for linear stability.

The evolution of one dimensional maps can be visualised by *cobweb diagrams* where $P\left(x\right)$ is plotted as a function of x. By plotting the identity line along with the map, each iterate corresponds to a vertical line to the map function followed by a horizontal line to the identity line. A fixed point manifests as a crossing of the map function with the identity line. A cobweb diagram around the fixed point can then be used to determine the stability properties of the map, even for nonlinear ones. See Figure 2.2 for illustrations of cobweb diagrams close to fixed points.

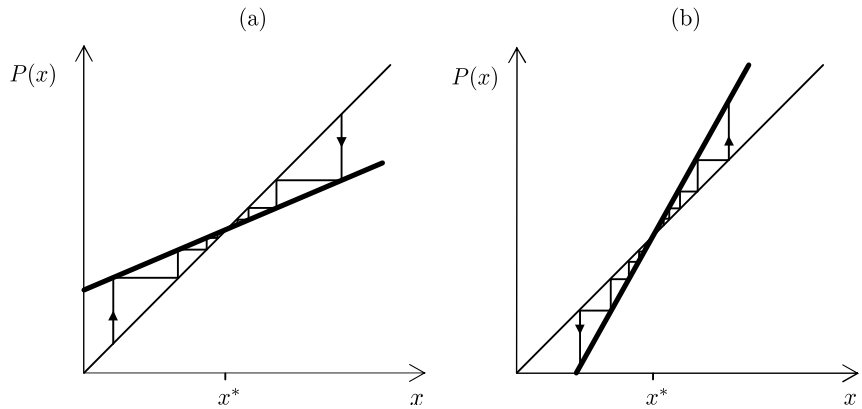

Figure 2.2: Cobweb diagrams of a map $P(x)$ (thick line) together with the identity line (thin line). In panel (a) $|P_{,x}(x)| < 1$ and thus the fixed point x^* asymptotically stable. In panel (b) $P_{,x}(x) > 1$ and thus x^* unstable.

2.4.4 Local stability and Poincaré maps

Local stability, i.e. how sensitive a periodic solution is to small perturbations, is a focus of this thesis. To examine the stability of a periodic solution of a smooth system, consider the flow $\mathbf{\Phi}$. For a periodic orbit it follows that $\mathbf{\Phi}\left(\mathbf{x}^*, T\right) = \mathbf{x}^*$ for some constant T. The local stability of a periodic trajectory based at the point $\mathbf{x}^*$ can be investigated to first order by the linearization of the flow around that trajectory:

$$\mathbf{\Phi}\left(\mathbf{x}, t\right) = \mathbf{\Phi}\left(\mathbf{x}^*, t\right) + \mathbf{\Phi}_{,\mathbf{x}}\left(\mathbf{x}^*, t\right) \cdot \left(\mathbf{x} - \mathbf{x}^*\right) + \mathcal{O}\left(\left(\mathbf{x} - \mathbf{x}^*\right)^2\right). \tag{2.16}$$

It follows that to investigate stability, it is necessary to find the *Jacobian* $\mathbf{\Phi}_{,\mathbf{x}}(\mathbf{x}^*, t)$. To do this, differentiate Equation 2.3 with respect to $\mathbf{x}$ and evaluate at $\mathbf{x}^*$:

$$\begin{array}{c} \mathbf{\Phi}_{,t\mathbf{x}}(\mathbf{x}^*, t) = \mathbf{f}_{,\mathbf{x}}(\mathbf{\Phi}(\mathbf{x}^*, t)) \cdot \mathbf{\Phi}_{,\mathbf{x}}(\mathbf{x}^*, t) \\ \mathbf{\Phi}_{,\mathbf{x}}(\mathbf{x}^*, 0) = \mathbf{Id} \end{array} . \tag{2.17}$$

The differential equation in Equation 2.17 is called the *first variational equation.* The initial value problems in Equation 2.3 (for $\mathbf{x} = \mathbf{x}^*$) and Equation 2.17 can now be solved simultaneously to find the flow $\mathbf{\Phi}$ and its Jacobian $\mathbf{\Phi}_{,\mathbf{x}}$. The flow function and its Jacobian can rarely be found explicitly, but they can be found by numerical simulations, see Section 2.7.

It is most convenient to study stability of periodic orbits on some hypersurface, $\mathcal{P}$, in state space, which the periodic trajectory intersects transversally. Such a surface is called a *Poincaré section.* Associate with $\mathcal{P}$ a map, $\mathbf{P}(\mathbf{x})$, called a *Poincaré map,* which takes points on $\mathcal{P}$ and maps them back to a subsequent intersection of $\mathcal{P}$. By the use of Poincaré maps the problem of stability of a periodic orbit is converted to a problem of fixed points of the Poincaré map. Specifically, let $\mathbf{x}^*$ be a point on $\mathcal{P}$, then $\mathbf{x}^*$ is a fixed point of $\mathbf{P}$ if $\mathbf{P}(\mathbf{x}^*) = \mathbf{x}^*$. In order to calculate the linearization of $\mathbf{P}$ around $\mathbf{x}^*$ let $\mathcal{P}$ be defined by the zero level of the smooth, scalar, event function $h_{\mathcal{P}}(\mathbf{x})$, i.e.

$$h_{\mathcal{P}}(\mathbf{x}) = 0. \tag{2.18}$$

Furthermore, the Poincaré map can be defined in terms of the flow function as

$$\mathbf{P}(\mathbf{x}) = \mathbf{\Phi}(\mathbf{x}, \tau(\mathbf{x})) \tag{2.19}$$

where $\tau(\mathbf{x})$ is the time-of-flight from the point $\mathbf{x}$ on $\mathcal{P}$ until the next crossing of $\mathcal{P}$ in the vicinity of $\mathbf{x}^*$, i.e. $h_{\mathcal{P}}(\mathbf{x}) = h_{\mathcal{P}}(\mathbf{\Phi}(\mathbf{x}, \tau(\mathbf{x}))) = 0$. Since $\mathcal{P}$ is crossed transversally by the periodic orbit the *implicit function theorem* (see [31]) guarantees that $\tau(\mathbf{x})$ exists, is smooth and unique in a neighbourhood of $\mathbf{x}^*$. It follows that

$$\begin{aligned} \mathbf{P}_{,\mathbf{x}}(\mathbf{x}^*) &= \left. \frac{d}{d\mathbf{x}} \mathbf{\Phi}(\mathbf{x}, \tau(\mathbf{x})) \right|_{\mathbf{x}=\mathbf{x}^*} && (2.20) \\ &= \mathbf{\Phi}_{,\mathbf{x}}(\mathbf{x}^*, T) + \mathbf{\Phi}_{,t}(\mathbf{x}^*, T) \cdot \tau_{,\mathbf{x}}(\mathbf{x}^*) && (2.21) \\ &= \mathbf{\Phi}_{,\mathbf{x}}(\mathbf{x}^*, T) + \mathbf{f}(\mathbf{x}^*) \cdot \tau_{,\mathbf{x}}(\mathbf{x}^*). && (2.22) \end{aligned}$$

Since $h_{\mathcal{P}}(\mathbf{\Phi}(\mathbf{x}, \tau(\mathbf{x}))) \equiv 0$ in a neighbourhood of $\mathbf{x}^*$, differentiation of $h_{\mathcal{P}}$ with respect to $\mathbf{x}$ gives

$$h_{\mathcal{P},\mathbf{x}}(\mathbf{x}^*) \cdot [\mathbf{\Phi}_{,\mathbf{x}}(\mathbf{x}^*, T) + \mathbf{\Phi}_{,t}(\mathbf{x}^*, T) \cdot \tau_{,\mathbf{x}}(\mathbf{x}^*)] = 0 \tag{2.23}$$

$$\Rightarrow \tau_{,\mathbf{x}}(\mathbf{x}^*) = -\frac{h_{\mathcal{P},\mathbf{x}}(\mathbf{x}^*) \cdot \mathbf{\Phi}_{,\mathbf{x}}(\mathbf{x}^*, T)}{h_{\mathcal{P},\mathbf{x}}(\mathbf{x}^*) \cdot \mathbf{f}(\mathbf{x}^*)}. \tag{2.24}$$

Substituting Equation 2.24 into Equation 2.22 yields

$$\mathbf{P}_{,\mathbf{x}}(\mathbf{x}^*) = \left[\mathbf{Id} - \frac{\mathbf{f}(\mathbf{x}^*) \cdot h_{\mathcal{P},\mathbf{x}}(\mathbf{x}^*)}{h_{\mathcal{P},\mathbf{x}}(\mathbf{x}^*) \cdot \mathbf{f}(\mathbf{x}^*)} \right] \cdot \mathbf{\Phi}_{,\mathbf{x}}(\mathbf{x}^*, T). \tag{2.25}$$

$\mathbf{P}_{,\mathbf{x}}(\mathbf{x}^*)$ can thus be calculated from known functions after $\mathbf{\Phi}_{,\mathbf{x}}(\mathbf{x}^*, T)$ has been found from the variational equation. Finally, the linearization of $\mathbf{P}$ locally to the point $\mathbf{x}^*$ is

$$\mathbf{P}(\mathbf{x}) \approx \mathbf{P}(\mathbf{x}^*) + \mathbf{P}_{,\mathbf{x}}(\mathbf{x}^*) \cdot (\mathbf{x} - \mathbf{x}^*) . \tag{2.26}$$

The stability problem of the periodic orbit has now been transformed into a stability problem of a fixed point for which the notions of stability and asymptotic stability are the same as for equilibrium points in **Definition 1**. From Equation 2.26 it follows that $\mathbf{P}_{,\mathbf{x}}(\mathbf{x}^*)$ governs how small disturbances from the periodic point $\mathbf{x}^*$ evolves. The Hartman-Grobman theorem tells us that if the eigenvalues (also known as the *characteristic-* or *Floquet multipliers*) of $\mathbf{P}_{,\mathbf{x}}(\mathbf{x}^*)$ are off the unit circle then the stability properties of the nonlinear system and its linearization are the same, locally to the fixed point [31]. Now, if the eigenvalues of $\mathbf{P}_{,\mathbf{x}}(\mathbf{x}^*)$ lie within the unit circle, then the closed orbit is linearly asymptotically stable. Conversely, if the largest eigenvalue is outside the unit circle the closed orbit is unstable. A borderline case is if the largest eigenvalue lies on the unit circle in which case a nonlinear stability analysis is required.

As $\mathbf{f}(\mathbf{\Phi}(\mathbf{x}^*, t))$ is a solution to the variational equation in Equation 2.17, it can be shown that $\mathbf{f}(\mathbf{x}^*)$ is an eigenvector to $\mathbf{\Phi}_{,\mathbf{x}}(\mathbf{x}^*, T)$ with associated eigenvalue one [37]. This is natural since a perturbation along the vector field of a periodic solution gets mapped to itself after one period. By multiplying Equation 2.25 with $\mathbf{f}(\mathbf{x}^*)$ it follows that $\mathbf{f}(\mathbf{x}^*)$ is also an eigenvector of $\mathbf{P}_{,\mathbf{x}}(\mathbf{x}^*)$ with associated eigenvalue zero. It can also be shown that the nontrivial eigenvalues of $\mathbf{P}_{,\mathbf{x}}(\mathbf{x}^*)$ coincide with those of $\mathbf{\Phi}_{,\mathbf{x}}(\mathbf{x}^*, T)$ [31]. The concept of Poincaré maps are explicitly used in **Papers B** and **C**.

An important result from the theory of piecewise-smooth systems is that a Poincaré map associated with an invariant set where the flow crosses all its discontinuity surfaces transversally (i.e. not tangentially) is still smooth. This implies that the above stability analysis still applies in those cases and also that all bifurcations of periodic orbits occurring in smooth systems can occur in piecewise-smooth systems as well.

In **Papers A, D** and **E** a closely related method is used to study stability. Here, perturbations away from a zero-velocity impacting, or grazing (see Section 2.6.2), orbit is studied. The fate of the perturbation is followed by means of Taylor series expansions of the flow function of the system. This can be achieved either directly if the analytical solution is known, which is the case for the one-degree-of-freedom systems studied in **Papers A, D** and **E,** or indirectly by implicit differentiation of some function of the flow with the aid of the implicit function theorem. Note that explicit solutions of piecewise-smooth dynamical systems are in practice usually impossible to find, however, if the dynamics is piecewise linear, analytical solutions can be found in subsets of state space where the dynamic equations are smooth. Similar types of stability analysis can be found in [38–40].

2.4.5 Structural stability

The above described notions of stability concerns the ultimate fate of the dynamics for perturbations of the initial conditions. *Structural stability* on the other hand, deals with perturbation of the system itself, i.e. perturbations of $\mathbf{f}(\mathbf{x})$, including parameter variations. Loosely speaking a smooth system is said to be structurally stable if small changes of the system retains the number and stability properties of the invariant sets of the system. For piecewise-smooth system the notion of structural stability is broadened to also encompass a preservation in the *event sequence*, i.e. the order and number of interactions with discontinuity surfaces. For a more rigorous definition of structural stability see [31].

2.5 Chaos

A special kind of invariant set of a dynamical system is a *chaotic attractor*. It is an attractor in the sense that the dynamics is actually contained to a subset of state space, albeit a complex one. Chaos is an intriguing phenomenon, not the least because of the beauty of the chaotic attractors and fractals, see e.g. [41,42]. Chaos is something which is indigenous to nonlinear dynamics, it can not occur in linear systems. The necessary condition for existence of chaos is that the dimension of the system is equal to or greater than three, and that it contains at least one nonlinearity. Possibly the simplest dynamical system exhibiting chaos is the Lorenz equation:

$$\dot{x} = \sigma(y - x) \tag{2.27}$$

$$\dot{y} = rx - y - xz \tag{2.28}$$

$$\dot{z} = xy - bz \tag{2.29}$$

where σ, r and b are parameters. Edward Lorenz derived this system in 1963 from a simplified model of convection rolls in the atmosphere [30]. He discovered that this simple deterministic system could show an extremely erratic behaviour for certain parameter values. However, he also found that the solution settled onto a complicated but bounded set, later named a *strange attractor*. This attractor is not a point, a curve nor a surface, it is a *fractal* with a dimension between 2 and 3.

A universally accepted definition of chaos does not exist but it is generally agreed that three criterion must be met for a response to be chaotic [30]:

1. Its steady-state response is aperiodic and erratic, i.e. it does not settle down to a fixed point or any kind of periodic or quasiperiodic orbit as $t \to \infty$.

2. The governing dynamical system is deterministic, i.e. the erratic response is not a product of noisy or random excitation but a product of the nonlinearities in the system.

3. The system has a sensitive dependence on initial conditions. That means nearby trajectories separate exponentially fast, which makes long term predictions of a future state impossible.

The last criterion can be checked by calculating what is called the *Lyapunov exponent* of the system [30].

Most engineering systems are designed to operate away from chaotic responses because of their unpredictability. However, chaotic responses might not always be disadvantageous. For example, it could very well be that the chaotic attractor has a maximum amplitude which is less than the maximum amplitude of a periodic response, which would be favourable in some engineering systems.

2.6 Bifurcations

As mentioned earlier the number and stability properties of the invariant sets of a dynamical system are of major importance when studying dynamical systems. For smooth systems a *bifurcation* is usually defined as a change in the number or stability properties of the invariant sets as a parameter (for example the amplitude or frequency of the excitation) of the system is varied, and the corresponding point in parameter space is called the *bifurcation point*. Or, in other words, at a bifurcation point the structural stability of the system is lost. For piecewise-smooth systems the definition of a bifurcation is broadened to encompass changes in the event sequence, a so-called *discontinuity-induced bifurcation* (DIB). A DIB usually, but not necessarily, also implies a change in number or stability properties of the invariant sets of the system. A *bifurcation diagram* is a plot of some measure of the invariant sets of a dynamical system against one of its parameters. A curve of solutions in a bifurcation diagram is called a *branch*.

There are numerous different bifurcations of smooth systems, see for example [30]. The simplest and most common one is the saddle-node bifurcation in which two coexisting fixed points, one stable and one unstable, meet and annihilate each other. After the bifurcation, no fixed point exists locally to the bifurcation point. See Figure 2.3(a) for a principal bifurcation diagram where a saddle-node bifurcation is marked. In this case the bifurcation occurs as the upper stable branch is followed for a decreasing parameter of the system. Saddle-node bifurcations can occur for both fixed points of differential equations as well as for periodic orbits, in which the described behaviour occurs for the fixed points of an associated Poincaré map. All types of bifurcations of smooth systems can also occur in piecewise-smooth systems, but as mentioned above there are also new types of bifurcations which can occur, the DIB's, see for example [31, 43]. This thesis concerns one type of DIB, namely the grazing bifurcation, discussed below.

2.6.1 Bifurcation scenarios

Bifurcations can be divided into two different groups depending on the scenario as the bifurcation point is crossed. If there exists a stable solution locally to the bifurcation point after the crossing, the scenario shows *persistence of a local attractor*. This implies that changes in the dynamics is gradual at the bifurcation, and the scenario is in that sense stable. For smooth systems, the transcritical bifurcation and supercritical versions of the pitchfork, Hopf and period-doubling bifurcations have this property. Figure 2.3(b) shows a principal bifurcation diagram of the impact-oscillator with friction from **Papers D** and **E** with this scenario.

On the other hand, if there exists no stable solution locally to the bifurcation point after the crossing, the scenario shows a *loss of a local attractor*. This is a scenario that is much more violent than the former case, since at the bifurcation the steady-state dynamics transitions to an attractor which is non-local to the bifurcation point. For DIB's this case is sometimes called a *non-smooth fold*. This scenario typically also exhibits hysteresis as the bifurcation parameter is varied around the bifurcation point. For smooth systems the saddle-node as well as the subcritical pitchfork, Hopf and period-doubling bifurcations have this property.

Grazing bifurcations can exhibit both scenarios depending on the parameters of the system. Figure 2.3(a) shows an example of a loss of a local attractor at the bifurcation point together with the associated hysteresis effect.

2.6.2 Grazing bifurcations

A *grazing bifurcation* occurs when the trajectory of a periodic solution tangentially intersects (grazes) some discontinuity surface in the state space of a piecewise-smooth system. This discontinuity surface can be of any type; a jump in state, vector field or one of its derivatives. However, in this thesis the term grazing bifurcation shall always mean a graze of a discontinuity surface where the state jumps, i.e. an impact occurs.

The low-velocity impacts that occur close to a grazing bifurcation point are severely destabilizing to the dynamics as they incur a square root singularity into the dynamics at the bifurcation point. To unfold the bifurcation it is necessary to first study what a low-velocity impact implies for the system response. To do this Nordmark derived the discontinuity map for grazing impacts [16]. The idea is to capture the effect of the impact as *a correction to the smooth dynamics* by applying a map at a suitable Poincaré surface in state space. To this end, assume that the vector field is smooth locally to the grazing point $\mathbf{x}^*$, and let the discontinuity boundary at which impacts occur be defined by the scalar

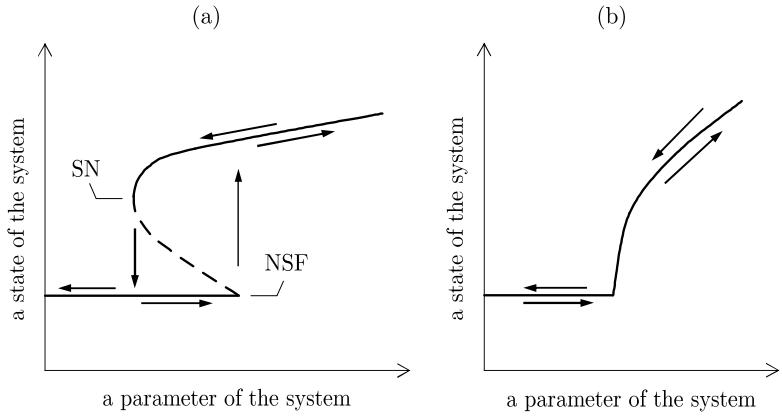

Figure 2.3: Principal bifurcation diagrams (of the impact-oscillator with friction from **Papers D** and **E**) with some measure of the state as a function of a parameter of the system. Solid lines correspond to stable solutions and dashed lines to unstable solutions. Panel (a) shows a scenario with loss of a local attractor at the non-smooth fold (NSF). As the parameter is increased past the bifurcation point the dynamics jumps to the upper branch. When the parameter is decreased the upper branch terminates in a saddle-node bifurcation (SN) for a parameter value below the NSF which shows the hysteresis effect. Panel (b) shows a bifurcation scenario with persistence of a local attractor.

function $h_{impact}(\mathbf{x}) = 0$. The definition of a grazing impact is then that

$$h_{impact}(\mathbf{x}^*) = 0 \tag{2.30}$$

$$h_{impact,\mathbf{x}}(\mathbf{x}^*) \cdot \mathbf{f}(\mathbf{x}^*) = 0 \tag{2.31}$$

$$\left(h_{impact,\mathbf{x}}(\mathbf{x}^*)\,\mathbf{f}(\mathbf{x}^*)\right)_{,\mathbf{x}} \cdot \mathbf{f}(\mathbf{x}^*) \stackrel{def}{=} a^* > 0 \tag{2.32}$$

where the first condition assures contact and the second condition that the contact occurs with zero relative velocity. The last condition is a condition on the relative acceleration, which means that the grazing trajectory is a parabola with a minima at $\mathbf{x}^*$. The impact surface is a candidate to define the discontinuity map on (see for example **Paper A**), however, it is usually not a wise choice as some trajectories nearby the grazing trajectory does not cross the impact surface. Instead, a natural choice is the surface defined by $h_{turning}(\mathbf{x}) \stackrel{def}{=} h_{impact,\mathbf{x}}(\mathbf{x}) \cdot \mathbf{f}(\mathbf{x}) = 0$ which corresponds to all points with zero relative velocity. This surface serves as a Poincaré section for the smooth vector field as all trajectories nearby to the grazing trajectory crosses this surface transversally. The problem with this surface is that trajectories that impact never reach this Poincaré section. The trick is thus to neglect the presence of the impact surface and let all trajectories flow to the Poincaré surface, apply the discontinuity map which transfers the state to another point on the Poincaré surface in a manner

which accounts for the impact, and then let the trajectories follow the smooth flow again. The steps are illustrated in Figure 2.4.

The discontinuity map is derived as follows. First the flow reaches point $\mathbf{x}_{in}$ at which the impact occurs. Instead of applying the impact map, the trajectory is allowed to proceed to the virtual point $\mathbf{x}_1$ on the Poincaré surface with $h_{impact}(\mathbf{x}) < 0$. The first of three steps in calculating the discontinuity map is then to flow backwards in time and calculate the point $\mathbf{x}_{in}$ by Taylor expansion of the flow around the grazing point $\mathbf{x}^*$. The next step is to apply the impact map $\mathbf{g}(\mathbf{x})$ on $\mathbf{x}_{in}$ to arrive at the point $\mathbf{x}_{out}$. The final step is to flow backwards in time along the smooth flow and calculate the virtual point $\mathbf{x}_2$ by Taylor expansion of the flow around $\mathbf{x}^*$. The discontinuity map is then the map from $\mathbf{x}_1$ to $\mathbf{x}_2$. See the illustration in Figure 2.4 for an overview of the trajectories and associated points. Detailed derivations of the discontinuity map can for example be found in [31] or [44]. To lowest order the discontinuity map is then

$$\mathbf{x} \mapsto \begin{cases} \mathbf{x} & h_{impact}(\mathbf{x}) \geq 0 \\ \mathbf{x}^* + \boldsymbol{\beta}\sqrt{-h_{impact,\mathbf{x}}(\mathbf{x}^*) \cdot (\mathbf{x} - \mathbf{x}^*)} & h_{impact}(\mathbf{x}) < 0 \end{cases}, \tag{2.33}$$

where

$$\boldsymbol{\beta} = \sqrt{\frac{2}{a^*}} \left(\frac{1}{a^*} \mathbf{f}(\mathbf{x}^*) \cdot h_{turning,\mathbf{x}}(\mathbf{x}^*) - \mathbf{I} \right) \cdot \mathbf{g}_{,\mathbf{x}}(\mathbf{x}^*) \cdot \mathbf{f}(\mathbf{x}^*) \tag{2.34}$$

and a^* is defined in Equation 2.32.

For $h_{impact}(\mathbf{x}) \geq 0$ the map is just the identity, since these points are not impacting. For $h_{impact}(\mathbf{x}) < 0$ points get mapped in the direction of $\boldsymbol{\beta}$ an amount which is proportional to the square root of the distance to the impact surface. Note that the map is continuous across $\mathbf{x}^*$ but the square root implies that the derivative of the map goes to infinity as $\mathbf{x} \to \mathbf{x}^*$ from the impacting side. This is the cause of the instability associated with grazing impacts. In contrast, a corresponding discontinuity map for a transversal crossing of an impact surface (a 'hard' impact) is linear to lowest order.

To describe the dynamics of a complete cycle of the periodic orbit the discontinuity map is concatenated with the smooth flow. A smooth flow is to the lowest order linear so the square root singularity is retained for the composite map.

Iterates of the composite map can then be studied to unfold the grazing bifurcation. It has for example been shown that the largest in magnitude eigenvalue of the Jacobian of the smooth flow determines whether the post grazing dynamics is periodic or chaotic in the persistence scenario [31]. An important result for the discussion in **Paper B** is a condition derived in [19] which determines whether the bifurcation scenario is persistent. Namely, if the sequence

$$h_{impact,\mathbf{x}}(\mathbf{x}^*) \cdot (\mathbf{P}_{smooth,x}(\mathbf{x}^*))^n \cdot \boldsymbol{\beta} > \mathbf{0},\ n = 1, 2 \ldots \infty \tag{2.35}$$

where $\mathbf{P}_{smooth,\mathbf{x}}$ is the Jacobian of the smooth vector field, then the ensuing bifurcation scenario shows persistence. The condition essentially means

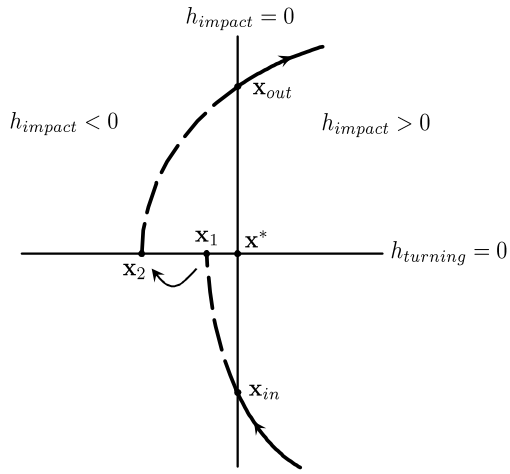

Figure 2.4: Illustration of the usage of the discontinuity map. The trajectory is continued passed the point of impact, $\mathbf{x}_{in}$, to the virtual point $\mathbf{x}_1$ on $h_{turning} = 0$. The discontinuity map is applied to take $\mathbf{x}_1$ to the point $\mathbf{x}_2$ on $h_{turning} = 0$. As the flow is resumed, the trajectory passes through the correct outgoing point $\mathbf{x}_{out}$ on $h_{impact} = 0$. $\mathbf{x}^*$ is the grazing point of the reference trajectory.

that for a perturbation such that an impact occurs, iterates of $\boldsymbol{\beta}$ under the smooth map gets mapped to the non-impacting side of the Poincaré section where $h_{impact}(\mathbf{x}) > 0$ for all future iterates. A necessary condition for this is that the largest in magnitude eigenvalue of $\mathbf{P}_{smooth,\mathbf{x}}$ is real and positive.

A comment should be made on the assumption that the vector field is smooth in the derivation of the discontinuity map. If the vector field is of Filippov type, like the friction oscillator in **Papers D** and **E**, then the dynamics might have sliding solutions in the neighbourhood of the grazing point. This makes it not straightforward to derive a discontinuity map since the flow in backwards time might contain sliding sections which makes the trajectory non-unique. That is why an explicit discontinuity map is not derived in **Papers D** and **E**. Instead the evolution in forward time of a perturbation from the grazing trajectory is studied.

2.7 Numerics

All numerical simulations in this thesis, i.e. numerical integration of initial value problems, was performed with an adaptive 4-th and 5-th order Runge-Kutta-Dormand-Prince method [45], implemented in the built-in Matlab [46]

function *ode45*. It was chosen since it is an efficient solver for non-stiff numerical problems.

When computing bifurcation diagrams, the terminal state of the system for one parameter value is chosen to be the initial condition for the next parameter value, to suppress transient dynamics and to remain on the same branch of the solution.

For numerical simulation of piecewise-smooth systems it is essential to record the transitions through the discontinuity surfaces, i.e. at impacts or switches between different vector fields of the system. Such transitions are called *events* and are triggered by zero crossings of scalar valued event functions. Matlab solvers (such as *ode45*) nowadays contain built in routines for detecting zero crossings of event functions with high accuracy, and have therefore been used here.

Of particular interest in **Papers B** and **C** are the eigenvalues of $\mathbf{P}_{,\mathbf{x}}$ of periodic orbits which have to be calculated numerically. This is done by starting with a set of initial conditions, $\mathbf{x}^*$, of the periodic orbit on a suitable Poincaré surface. By forward simulation, the variational equations in Equation 2.17 can then be integrated until the next crossing of the Poincaré surface. $\mathbf{\Phi}_{,\mathbf{x}}$ is then projected onto the Poincaré surface by Equation 2.25 to get $\mathbf{P}_{,\mathbf{x}}$. However, discontinuities in the system dynamics has to be taken account of during the numerical integration. Let $\mathbf{\Phi}^{in}_{,\mathbf{x}}$ be the state of the solution to the variational equations at the transversal crossing of a discontinuity surface defined by the event function h. Let $\mathbf{f}_{in}$ be the vector field of the incoming trajectory, $\mathbf{f}_{out}$ the vector field of the outgoing trajectory, $\mathbf{g}$ a jump map defined on the discontinuity surface and $\mathbf{x}_{in}$ the point of crossing. In the numerical script the integration is stopped at $h(\mathbf{x}_{in}) = 0$, the initial conditions for the variational equation is then updated to

$$\mathbf{g}_{,\mathbf{x}}(\mathbf{x}_{in}) \cdot \left[\mathbf{Id} - \frac{\mathbf{f}_{in}(\mathbf{x}_{in}) \cdot h_{,\mathbf{x}}(\mathbf{x}_{in})}{h_{,\mathbf{x}}(\mathbf{x}_{in}) \cdot \mathbf{f}_{in}(\mathbf{x}_{in})}\right] \cdot \mathbf{\Phi}^{in}_{,\mathbf{x}}, \tag{2.36}$$

and then the integration is continued with the vector field $\mathbf{f}_{out}$. See [47] for a thorough derivation.

Naturally, direct simulation of periodic trajectories is only possible for those that are stable. However, a root-finding method, such as the Newton-Raphson method can be used to locate unstable periodic solutions. A branch of such solutions can then be followed by numerical *continuation*, see for example [23] and references therein.

Chapter 3

Mechanical models

This work investigates mechanical systems with two particular features: recurrent dynamics and impacts. This class of dynamical systems are usually referred to as *impact oscillators* or *vibro-impact systems*. Additionally, this work is focused on detailed studies of impact dynamics, and systems with few degrees-of-freedom, for which the event driven approach described in the previous section is a suitable method of analysis. The governing dynamical equations of motion are derived from Newton's second law

$$\sum_i F_i = m\ddot{x}, \tag{3.1}$$

where the F_i-s are the external forces acting on an object with mass m and $\ddot{x}$ is the acceleration of the object.

As an example, consider the one-degree-of-freedom impact oscillator in Figure 3.1(a). A version of this impact oscillator is investigated in **Paper B**. Here, the object with mass m is attached to a rigid, but forced, frame via a linear spring with spring constant k and a linear damper with damping constant d. The external forces acting on the object is thus the spring and damper forces. The spring force is proportional to the compression distance of the spring and the damper force is proportional to the compression velocity of the damper. If x denotes the position of the object relative to its neutral position with a relaxed spring, and $f(t) = a\sin\omega t$ is the position of the frame, the governing equation of motion is thus by Equation 3.1

$$-k\left(x - a\sin\omega t\right) - d\left(\dot{x} - a\omega\cos\omega t\right) = m\ddot{x}, \tag{3.2}$$

when the object is away from impact and where a and ω are constants and t is time. This differential equation is a linear system with periodic, time dependent forcing. By studying the system in Figure 3.1(a), the object will impact a rigid wall if $x = \delta$. The event function, whose zero-level defines contact between the object and wall, is thus $h_{impact} = \delta - x$, and the object is restricted to move in the subset $h_{impact} \geq 0$.

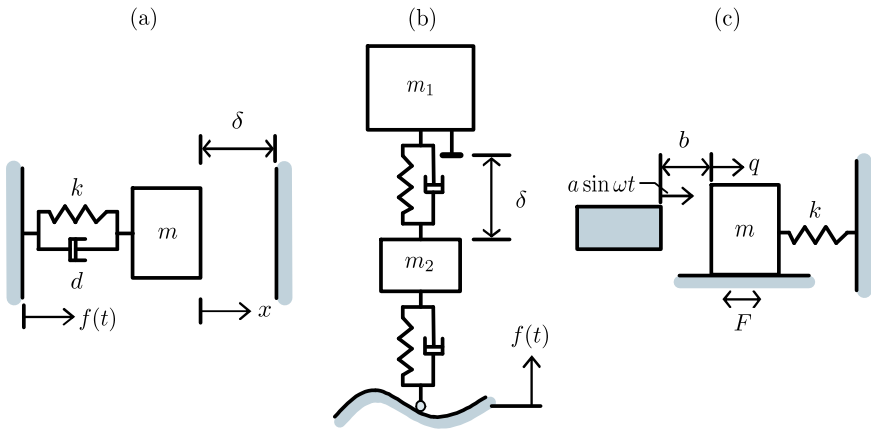

Figure 3.1: A one-degree-of-freedom impact oscillator (a), the quarter-car model (b), and the impact oscillator with friction (c). $f(t)$ is the forcing function and δ is the distance from object to wall in (a) and suspension clearance in (b), at the equilibrium position of the respective system without forcing. In (c), the forcing is explicitly stated as $a\sin\omega t$, and b is the distance between the object in the configuration with an undeformed spring and the average position of the forcing.

In **Paper C** is a simple model of a car known as the *quarter-car model* [48] investigated. A two-degree-of-freedom version is shown in Figure 3.1(b). This model is used to study vertical motion of the car, and it is therefore suitable for comfort studies. The assumption behind the model is that all four wheels are exposed to the same forcing, and thus that the mass of the four wheels and their suspensions can be lumped into one mass and one suspension. The upper mass represents the chassis and is often called the sprung mass as it rests on the suspension. The lower mass is consequently called the unsprung mass, and besides the wheels it consists of parts of the suspension and driveline which are unsupported by the suspension. The suspension and tire is here modelled as simple spring-damper systems.

The stiffness of the tire is typically an order of magnitude higher than the suspension stiffness, which makes the natural frequency of the sprung mass an order of magnitude lower than the natural frequency of the unsprung mass. For a passenger car it is often about 1 Hz for the sprung mass and about 10 Hz for the unsprung mass. The damping of the tire is small compared to the damping in the suspension and is often neglected.

The quarter-car model is usually modelled as a linear system, however, a real vehicle suspension is very much nonlinear. The damping is usually lower in the compression phase than in the expansion phase to increase comfort. This can typically be modelled as a bilinear damping with different damping constants

in expansion and compression. Another source of strong nonlinearity is the *wheel-hop* phenomenon where the wheel loses contact with the ground and the system assumes a free falling state; a situation often overlooked when modelling and simulating suspensions with wheel to ground contact. Finally, to cope with high amplitude excitations a suspension is always fitted with a *bumpstop,* marked as a stop in Figure 3.1(b), which is engaged at extreme compressions of the suspension. These are large rubber or polyurethane bushings which acts as extremely stiffening springs. Their purpose is to protect the suspension, chassis and passengers from hard impacts which could be damaging to the construction and extremely uncomfortable for humans. Some examples of research focusing on models including bumpstops and wheel hop are [10, 49, 50].

Forcing of the quarter-car model is due to interaction of the tire with the ground when the vehicle has a non-zero horizontal velocity. For comfort studies a periodic forcing is usually considered, and with the inclusion of the bumpstop the quarter-car model can thus be treated as an impact oscillator.

In **Papers D** and **E** an impact oscillator with dry-friction type damping is considered, shown in Figure 3.1(c). This model was chosen as it is the most simple type of impact oscillator since the mass spring system is only forced through impact interactions with an oscillating constraint. The equations governing the friction oscillator in absence of impacts is then

$$m\ddot{q} + kq = F \tag{3.3}$$

where q is the position of the object with mass m, k is the spring constant and F is the friction force

$$F = \begin{cases} -F_f & \text{when } \dot{q} > 0 \text{ or when } \dot{q} = 0 \text{ and } q > \frac{F_f}{k} \\ F_f & \text{when } \dot{q} < 0 \text{ or when } \dot{q} = 0 \text{ and } q < -\frac{F_f}{k} \\ kq & \text{when } \dot{q} = 0 \text{ and } |q| \leq \frac{F_f}{k} \end{cases} . \tag{3.4}$$

The position of the oscillating constraint is $-b+a\sin\omega t$ where a is the amplitude, ω the angular frequency and b the distance from the average position of the oscillating constraint to the object at the neutral position with an undeformed spring. Impacts, which occur if $q = -b+a\sin\omega t$, are modelled as instantaneous updates of the relative velocity,

$$\dot{q}|_{after} - a\omega\cos\omega t = -e\left(\dot{q}|_{before} - a\omega\cos\omega t\right), \tag{3.5}$$

where e is the coefficient of restitution and the constraint is assumed to be unaffected by the impact.

Chapter 4

Control

If a dynamical system shows unwanted dynamic behaviour some kind of control action can be applied to the system to improve the performance. For smooth systems the control action affects the vector field such that a general dynamical system with control is described by

$$\dot{\mathbf{x}} = \mathbf{f}(\mathbf{x}, \mathbf{u}), \mathbf{x} \in \mathbb{R}^n, \ \mathbf{u} \in \mathbb{R}^k. \tag{4.1}$$

Normally, *feedback control* is employed, where the the control input is a function of the state of the system, i.e. $\mathbf{u} = \mathbf{u}(\mathbf{x})$. The task of finding functions $\mathbf{u}(\mathbf{x})$ suitable for different control tasks is a huge field of research. See for example [51] for linear control strategies (linear control functions applied to linear dynamical systems) and [35] for smooth nonlinear control strategies.

4.1 Control of piecewise-smooth systems

Piecewise-smooth systems falls under the category of nonlinear systems and hence requires nonlinear analysis techniques. Researchers have primarily developed nonlinear control strategies for smooth systems since discontinuities adds difficulties to the analysis. Attempts at controlling piecewise-smooth systems are restricted to certain classes, and for specific control objectives. Many open control problems still exist, and a unified control theory will probably never be found, since piecewise-smooth systems include so diverse types of systems. In the following some examples of previous research in this area is presented.

For nonlinear systems, so-called *Lyapunov functions*, a type of generalized energy functions, can be used to prove asymptotic stability of fixed points. These functions can also be used to find stabilizing feedback control laws [35]. Brogliato and co-workers have extended the use of Lyapunov functions to find control laws for some classes of non-smooth systems including impacts, see for example [52]. A related approach is presented in [53], where the problem of stabilizing a system which includes impacts is recast as a problem of adaptive

regulation for a plant with parametric uncertainty, where the uncertainty parameter $\theta \in \{0, 1\}$ switches between the contact- and non-contact phases. A suitable Lyapunov function is here constructed by the use of the backstepping technique [35]. This Lyapunov function is then used to find a stabilizing control law. The backstepping method is however only applicable to nonlinear systems with a certain structure. In [54] a Lyapunov function is used to find a stabilizing control law for an idealized system of a mass on a moving belt which can exhibit friction induced self-excited vibrations. In this example the potential and kinetic energy can be used to construct the Lyapunov function. The control input is here assumed to be the normal load and the resulting control law is piecewise linear. Self-excited vibrations is a subject which has gained considerable attention since it is a common nuisance in systems such as brakes and controlled positioning systems of industrial production systems. Another example of control of non-smooth systems is to approximate the dynamics of a nonlinear system as continuous, but piecewise linear, in tracking control problems [55,56]. The governing equations of motion are then transformed into difference equations where time is discrete. Optimal controls, that take a number of future time steps into account, can then be found by using dynamic programming.

The above mentioned methods all rely on continuous input of control energy into the system, and in that regard resemble classical control strategies. In this work, however, the control strategies rely on discrete-in-time control inputs. This method is for example used in OGY-control which was introduced by Ott, Grebogi and Yorke in [57]. This control method is applicable to a system with chaotic response. Typically, a number of unstable periodic orbits are embedded in a strange attractor, and anyone of these could serve as candidates for stabilization. Also, as chaotic systems have a sensitive dependence on initial conditions, small (control) perturbations can have a substantial impact on the dynamics. The idea is to make small perturbations of one of the parameters of the system as the trajectory intersects a predefined Poincaré surface. A requirement of the unstable fixed point on this surface is that it is a saddle point, i.e. it has a stable and an unstable manifold associated with it. The other requirement is that an accessible parameter shifts the position of the fixed point. Ott, Grebogi and Yorke derived a control law, based on the eigenvalues and eigenvectors of the Poincaré map, that places the point of intersection of the trajectory on the stable manifold, which assures asymptotic stability of the fixed point. It is also shown that this method is suitable for experimental studies. In [58] the control strategy is implemented in an impact oscillator with friction. See also [59,60] for other interesting works on this method.

Another method with discrete control inputs, using a similar analysis technique as in the present work, is presented by Angulo et al. in [61]. They study how a limit cycle can be controlled by introducing a corner collision bifurcation. This type of bifurcation occurs when a limit cycle crosses a corner of a subset in state space. In this corner a different vector field applies and it is assumed that this vector field can be affected by a control input. By deriving a discontinuity map, which accounts for the correction to the dynamics induced by the

time spent in the controlled subset of state space, the local dynamics can be analysed. The discontinuity map is in this case piecewise linear. By choosing an appropriate control law the amplitude of the limit cycle can be controlled. As the time spent in the controlled subset of state space is short, the control effort is minimal.

Similarly to the two last examples above, the control strategies in this work is aimed at a very specific situation. Namely, to control the onset of low-velocity impacts. As mentioned above, the proposed control methods rely on discrete-in-time control inputs in order to be as energy efficient as possible. The idea is to make small shifts of the position of the impact surface to control the dynamics at a grazing bifurcation. See section 5.2 for a further discussion.

Chapter 5

The present work

This chapter presents the scientific contributions of the present work. The first section summarizes the appended papers, which contain the results of the research. The second section gives some more detail of the proposed control methods which are presented and used in **Papers B**, **C** and **E**. Finally, the third section contains two subsections with additions to the study in **Paper E**. The first subsection regards the bifurcation scenario for a more complicated friction model, and the second subsection discusses robustness of the proposed control strategy. These two subsections are not independent, and readers are referred to **Paper E** for the context and for definitions of variables and parameters.

5.1 Summary of appended papers

The first appended paper, **Paper A**, gives an experimental verification of the presence of a square root term in the discontinuity map of near grazing impacting dynamics in an impact oscillator. Specifically, it is shown that the transient growth rate of the impact velocity is proportional to the square root of the impact velocity in the previous cycle. An implication is thus that, as the impact velocity goes to zero, the growth rate goes to infinity. This shows that the grazing bifurcation is initially very fast compared to for example a saddle-node bifurcation. The experimental setup consists of a steel ball on a leaf spring rigidly clamped to a stand. Suitably positioned is an electromagnetical shaker whose head impacts the steel ball at a critical driving voltage. The velocity of the steel ball is measured with a laser vibrometer. The results of 20 runs for five different driving frequencies are shown and the results correspond very well with that of the theoretical predictions and numerical simulations.

In **Paper B** the question of stabilization by means of an active low-cost control is addressed. A discrete control algorithm is proposed to assure local persistence of an attractor around grazing impacts for n-dimensional impact oscillators with a smooth vector field. A proof is given for stabilization utilizing

the theory of discontinuity mappings, going back to the works of Nordmark and Fredriksson [16,19]. The proof is constructive in the sense that it provides tools for selecting stabilizing control parameters. Implementation of the control strategy is exemplified on one- and two-degree-of-freedom impact oscillators. The idea behind the control algorithm is to introduce a new discontinuity surface in state space which makes it possible to select one of the eigenvalues of the Jacobian of the Poincaré map. In this article it is highlighted that the application of the control map also changes the eigenvectors of the Jacobian of the Poincaré map. This fact is the basis for the constructive proof of stabilizability.

Paper C then implements this control algorithm in a two-degree-of-freedom quarter-car model, which is a simplified model of a vehicle for studying vertical motion. Here, the quarter-car model is set in the framework of piecewise-smooth systems to account for three different discontinuities. First, a bumpstop, which is a rubber bushing which is activated for large compressions of the suspension. Impacts with the bumpstop are modelled as rigid with an associated coefficient of restitution. Second, the damping in the suspension is modelled as piecewise linear with one damping constant in compression and one in expansion. Third, a possible loss of ground contact is accounted for by a change of differential equations at suitable discontinuity surfaces. A presence of damping in the tire is also accounted for which makes the tire-ground contact problem slightly complicated. In this case a quasi-contact phase has to be introduced where the normal force on the tire is zero even though the tire is not fully relaxed. The proposed control algorithm is then implemented in a successful way, proving that it can be applied also on dynamical systems with several discontinuities.

In **Papers D** and **E** the grazing bifurcation triggered by the disappearance of a steady-state stick, or sliding, solution of an example impact oscillator with Coulomb-friction type damping is investigated. In absence of impacts the friction force generates a set of relative equilibria, $\mathcal{S}_0$, with the mass in stick, $\dot{q} = 0$, and the position coordinate in the interval $[-F_f/k,\ F_f/k]$, with notation according to Section 3. $\mathcal{S}_0$ is then contained in the switching set $\mathcal{S} \stackrel{def}{=} \{\dot{q} = 0\}$ which separates motion with opposing directions of the friction force. Additionally, the set $\mathcal{I} \stackrel{def}{=} \{q = -b + a\sin\omega t\}$ defines the oscillating constraint and the motion of the object is thus restricted to $q \geq -b + a\sin\omega t$. In the state-space with coordinates $(q,\ \dot{q},\ \omega t \bmod 2\pi)$ the three sets can be visualized as in Figure 5.1, which shows three different configurations of the system. In the top panel of Figure 5.1 $a - b < F_f/k$ such that a part of $\mathcal{S}_0$ is unaffected by the oscillating constraint. This locally attracting and invariant subset of $\mathcal{S}_0$ contains the stick solutions in the form of straight-line trajectories, parallel to the phase axis. On the other hand, in the bottom panel, where $a - b > F_f/k$, no steady-state stick solutions exist and all trajectories must include impacts and phases with positive and negative slip of the object. In the bordering case $a - b = F_f/k$, shown in the middle panel of Figure 5.1, a single stick trajectory exists which has a tangential, or grazing, contact with $\mathcal{I}$. This is the critical configuration at which the grazing bifurcation occurs.

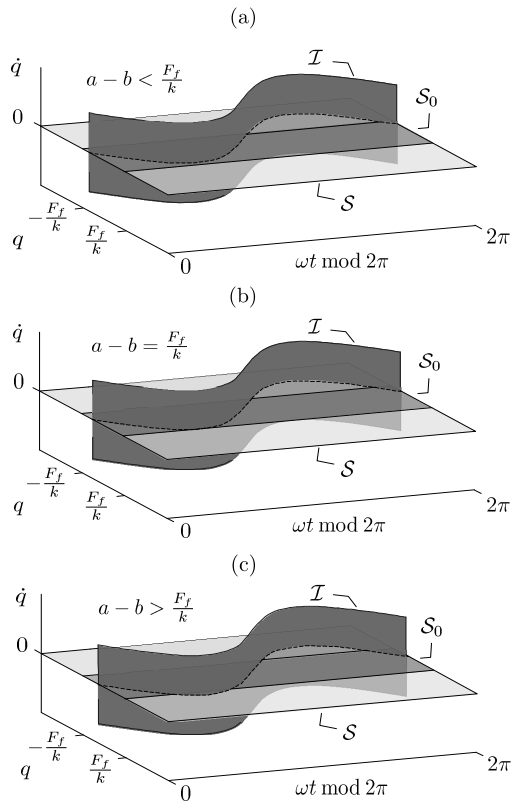

Figure 5.1: State space structure of the impact oscillator with friction in a configuration prior to grazing (a), at grazing (b) and subsequent to grazing (c). $\mathcal{I}$ is the impact surface, $\mathcal{S}$ is the surface where the friction force switches direction and $\mathcal{S}_0$ is the subset of $\mathcal{S}$ which contain straight line stick trajectories in the absence of impacts. Modification of original, reproduced with permission from [64].

In **Paper D,** under the assumption that the driving frequency is less than twice the natural frequency of the spring-mass system, small perturbations from the grazing trajectory are studied and from a lowest order analysis it is concluded that the condition

$$a^*\omega^2 < \frac{4F_f}{m\,(1+e)^2} \tag{5.1}$$

assures that the grazing trajectory is asymptotically stable, where a^* is the critical amplitude of the constraint. Simulations show that an asymptotically stable grazing trajectory implies a persistent attractor across the bifurcation point and a loss of a local attractor otherwise. Also, a two-degree-of-freedom system is simulated which corresponds to an oscillating constraint with finite mass. In the limit of infinite mass the stability properties of the grazing bifur-

cation is shown to agree with the one-degree-of-freedom system. As the mass of the constraint is reduced, the set of parameter values for a persistent attractor diminishes and for a mass ratio of about 100 seems to vanish altogether.

In **Paper E** a piecewise linear map is constructed from the analytical solutions of the system which captures the dynamics of the system. The above mentioned restriction on the driving frequency implies that the mass must reach the sliding surface before each impact. This simplifies the analysis since one dimension is lost on the sliding surface, and thus a one-dimensional map is sufficient to describe the dynamics. The map captures the dynamics in a neighbourhood around the bifurcation point, and it is thereby shown analytically that a stable branch of impacting periodic solutions emanates from the bifurcation point if Equation 5.1 is satisfied. An additional result is that the map shows that the near grazing dynamics is to lowest order linear in the deviation from the grazing point and not proportional to a square root of the deviation, as is the case for impact oscillators without the presence of a friction-induced sliding region. To illustrate this, Figure 5.2 shows a principal impacting trajectory. Starting with a perturbation from the boundary of the stick region of size ϵ in position, this perturbation gets stretched to a velocity of size $\sqrt{\epsilon}$ by the impact map. However, the smooth flow for positive velocity cancels the square-root singularity such that the perturbation in position at zero velocity is again of size ϵ. The ensuing flow for negative velocity is symmetric around the boundary of the stick region, preserving the ϵ-size perturbation.

Additionally, in **Paper E** low-cost control algorithms are derived, both linear and nonlinear, which assures a persistent attractor across the bifurcation point regardless of the parameter values of the system. The basic idea is the same as in **Papers B** and **C**, in which small corrections of the neutral position of the oscillating constraint is made at discrete moments away from impact. The control algorithms are based on feedback of the position of the mass in stick, as well as knowledge of the increase in amplitude past the grazing amplitude. By substitution of the position of the impact surface with a feedback control function, the stability of the ensuing dynamics is analysed by the same means as for the uncontrolled system.

The dynamics of the impact oscillator with friction has also been analysed in [62,63], and with inclusion of control in [64], by the present author and others.

5.2 Proposed control methods

As has been argued in previous sections, the onset of low-velocity impacts in a system with recurrent dynamics introduces a strong nonlinearity which might cause the system dynamics to bifurcate to a violent response because of a loss of a local attractor. Here, control strategies to overcome this problem is presented in **Papers B**, **C** and **E**. Particularly this is done by altering the bifurcation scenario from a loss- to persistence of a local attractor.

The proposed control strategies are based on two ideas:

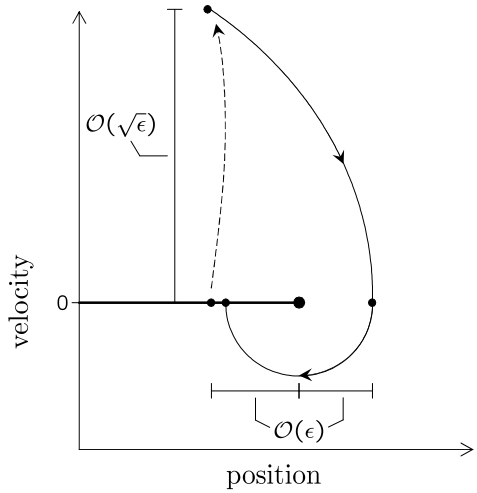

Figure 5.2: Principal impacting trajectory of the impact-oscillator with friction. The solid line at zero velocity represents the set $\mathcal{S}_0$ and the large dot represents the grazing trajectory. The figure illustrates that an ϵ-size perturbation from the grazing trajectory at the boundary of the stick region, is retained at the return to the stick region following an impact.

1. To explicitly utilize the impact nonlinearity for control actuation.

2. To leave the natural dynamics of the system as undisturbed as possible.

Actively controlling the dynamics of a system naturally requires energy, and it is therefore energy efficient to utilize the natural dynamics as much as possible. The control strategy is therefore termed *low-cost control* in the appended papers. The proposed control strategies are based on changing the geometry of the dynamical system, more precisely the position of the impact surface, away from impact, in order to time the impacts in a way such that stabilization is achieved. Thus, the vector field of the system is untouched, and the only energy consumption associated with the control is in repositioning the impact surface itself.

The control strategy of **Papers B** and **C** explicitly uses the Poincaré map description of the dynamics of impact oscillators. The idea is to introduce a new Poincaré section, $\mathcal{C}$, with an associated control map. Every time the trajectory intersects $\mathcal{C}$ the position of the impact surface, δ, is shifted by a small amount. The update law is the linear map

$$\delta \mapsto \delta^* + \mathbf{c} \cdot (\mathbf{x} - \mathbf{x}^*) + c_0 (\delta - \delta^*), \tag{5.2}$$

where $\mathbf{c}$ and c_0 are control parameters, and $\mathbf{x}^*$ is the fixed point on $\mathcal{C}$ associated with a trajectory that grazes an impact surface positioned at δ^*. By introducing δ as an additional state of the system it can be shown that c_0 is a Floquet multiplier of the controlled system dynamics while the rest of the multipliers are equal to those of the uncontrolled dynamics, given that the smooth dynamics is unaffected by δ. The task is then to choose the control parameters to satisfy the stability condition in Equation 2.35. This problem is addressed in **Paper B**.

This control strategy was introduced in [44]. See also [65] for an implementation of the control in an impact microactuator. Previously, the same basic idea has been implemented in systems with hard impacts exemplified by a hopping robot, a Braille printer and a bipedal walker [47, 66]. In those cases the stability analysis is a more straightforward matter of positioning the multipliers inside the unit circle, whereas in **Paper B**, the control parameters are used to align the eigenvectors of the Poincaré map of the controlled system to satisfy the stability condition in Equation 2.35.

The control strategy for the impact oscillator with friction in **Paper E** is based on the same idea as the one described above. Namely, to make small shifts of the position of the impact surface at discrete moments in time when the system is away from impact to ensure a bifurcation scenario with persistence of a local attractor. The derivation of the control law is based on the analysis of the system without control. For this case, a piecewise linear map in x which captures the near grazing dynamics is derived. The value of x in the map corresponds to the position of the mass at each crossing of the switching surface $\mathcal{S}$. A linear update law of the form

$$\tilde{b}\,(x, \tilde{a}) = \tilde{a}^* - 1 + (1 - c_{\tilde{a}})\,(\tilde{a} - \tilde{a}^*) + \left(1 - \frac{2c_x}{\gamma}\right)(1 - x)\,, \tag{5.3}$$

where $\tilde{b}$ is the neutral position of the forcing in non-dimensional coordinates, $x = \frac{k}{F_f} q$ is the position of the mass at the crossing of $\mathcal{S}$, $\tilde{a} = a\frac{k}{F_f}$ is the amplitude of the forcing, $\tilde{a}^* = a^* \frac{k}{F_f}$ is the grazing amplitude, $c_{\tilde{a}} > 0$ and $c_x > 0$ are control parameters and $\gamma = \frac{ma^*\omega^2(1+e)^2}{2F_f}$, substituted into the map then corresponds to making small shifts in $\tilde{b}$ at each crossing of the switching surface ($\tilde{a} \approx \tilde{a}^*$ and $x \approx 1$ close to the bifurcation point). From the map it can be concluded that a local attractor persists at the grazing bifurcation if $c_x < 1$.

5.3 Additions to Paper E

5.3.1 Bifurcation scenarios with improved friction model

In **Papers D** and **E** it was assumed that the static and dynamic friction coefficients were equal. In reality the static friction coefficient is typically larger than the dynamic friction coefficient and it is therefore of interest to investigate the

associated bifurcation scenario and to compare it to the scenarios in **Papers D** and **E**. The analysis in **Paper E** lends itself to a straightforward qualitative analysis for this case. The motion in absence of impacts is then again defined by Equation 3.3 but with

$$F = \begin{cases} -F_d & \text{when } \dot{q} > 0 \text{ or when } \dot{q} = 0 \text{ and } q > \frac{F_s}{k} \\ F_d & \text{when } \dot{q} < 0 \text{ or when } \dot{q} = 0 \text{ and } q < -\frac{F_s}{k} \\ kq & \text{when } \dot{q} = 0 \text{ and } |q| \leq \frac{F_s}{k} \end{cases} \tag{5.4}$$

where F_s is the static friction coefficient, F_d is the dynamic friction coefficient and $F_s > F_d$. This implies that trajectories in state space ($\dot{q}$ versus q) for $\dot{q} \neq 0$ are segments of ellipses centred around $-\frac{F_d}{k}$ for $\dot{q} > 0$, and $\frac{F_d}{k}$ for $\dot{q} < 0$. However, the stick region, where $\dot{q} = 0$, is not in the interval between these points as if $F_d = F_s$, but instead in the interval $-\frac{F_s}{k} \leq q \leq \frac{F_s}{k}$. As in **Paper E**, let the position of the oscillating constraint be $q_c = -b + a \sin \omega t$ where b, a and ω are constants and restrict attention to the neighbourhood of $q = \frac{F_d}{k}$. Let $a^* = b + \frac{F_d}{k}$ and $a^{**} = b + \frac{F_s}{k}$. Then a^* and a^{**} is the amplitude at which the oscillating constraint has its maximum position at $\frac{F_d}{k}$ and $\frac{F_s}{k}$ respectively. Then, for F_s sufficiently close to F_d the analysis of the dynamics and stability of fixed points in **Paper E** still holds, for all trajectories that do not reach the set $\mathcal{R} \stackrel{def}{=} \left\{ \frac{F_d}{k} < q \leq \frac{F_s}{k}, \dot{q} = 0 \right\}$. Trajectories in $\mathcal{R}$ either remains in $\mathcal{R}$ as stick trajectories or possibly leaves $\mathcal{R}$ through an impact. Note that trajectories can only reach $\mathcal{R}$ from the set $\dot{q} > 0$. We can now deduce the nature of possible steady state trajectories in the vicinity of $q = \frac{F_d}{k}$ by studying the four cases in Figure 5.3.

Figure 5.3(a) shows example trajectories when $a \lesssim {}^1 a^*$. As the analysis in **Paper E** shows, if the opposite inequality of Equation 5.1 holds there is an unstable and a stable steady state impacting trajectory for a less than and sufficiently close to a^* if $F_d = F_s$. If one or both of these trajectories behave like $\mathbf{\Phi}_1$ they would still exist if $F_s > F_d$, but if they behave like $\mathbf{\Phi}_2$ they do not. An initial condition on $\mathbf{\Phi}_2$ would simply end up as a stick trajectory. In Figures 5.3(b)-(d) $a \geq a^*$ and we restrict attention to the case where the inequality of Equation 5.1 is satisfied, since this is the only case when steady state impacting trajectories exist locally to $q = \frac{F_d}{k}$. In Figure 5.3(b) $a = a^*$. In this situation $\mathbf{\Phi}_1$ solutions do not exist in steady state since it is shown in **Paper E** (and **D**) that these are attracted towards the point $\left\{ q = \frac{F_d}{k}, \dot{q} = 0 \right\}$ and consequently end up as stick solutions. $\mathbf{\Phi}_2$-type trajectories also end up as stick solutions. In Figure 5.3(c) we have $a^* \lesssim a \lesssim a^{**}$. In this case $\mathbf{\Phi}_1$ steady state solutions exist if a is sufficiently close to a^{**}. If not, a steady state solution for $F_s = F_d$ would here be a $\mathbf{\Phi}_2$ solution and end up as a stick trajectory. The value of a for when $\mathbf{\Phi}_1$ solutions exist could be calculated from the explicit expressions of the map of the dynamics in **Paper E**. At the same time, the stick solutions in the set $\left\{ a - b \leq q \leq \frac{F_s}{k}, \dot{q} = 0 \right\}$ still exist. Finally, consider Figure 5.3(d) where

[1] $\lesssim$ is here defined as $<$ and $\approx$.

$a^{**} \lesssim a$. In this case no stick solutions remain, and the only local steady state solution is an impacting trajectory of type $\mathbf{\Phi}_2$.

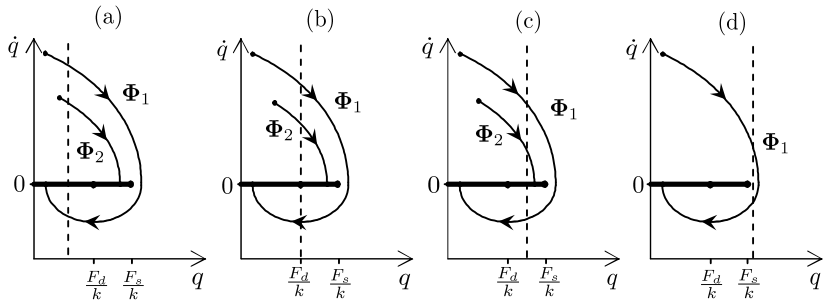

Figure 5.3: Example trajectories for different forcing amplitudes. The dashed line corresponds to the maximum position of the oscillating constraint. In (a) $a \lesssim a^*$, in (b) $a = a^*$, in (c) $a^* \lesssim a \lesssim a^{**}$ and in (d) $a^{**} \lesssim a$.

Figure 5.4(a) shows a qualitative bifurcation diagram for when the opposite inequality of Equation 5.1 holds and the unstable branch of solutions is here nonexistent for an interval of a close to a^*. Besides this property, another difference from the bifurcation diagram in Figure 2.3(a) is that the interval of stick solutions is increased to $a = a^{**}$. Figure 5.4(b) shows a typical bifurcation diagram for when the inequality of Equation 5.1 is satisfied. Then the interval of stick solutions is again increased to $a = a^{**}$ compared to Figure 2.3(b). In addition, an interval of the stable impacting steady state solutions has disappeared compared to Figure 2.3(b). The interesting thing to note here is that if $F_s > F_d$ there is a jump and a hysteresis effect in the bifurcation scenario even if Equation 5.1 is satisfied, although the interval of hysteresis is typically smaller than if Equation 5.1 is not satisfied.

5.3.2 Some notes on robustness of the control algorithm

To investigate the sensitivity of the proposed control strategies to multiplicative errors in the measurement data, consider the control law

$$\tilde{b}\,(x, \tilde{a}) = \tilde{a}^* - 1 + (1 - c_{\tilde{a}})\,(1 + \epsilon_1)\,(\tilde{a} - \tilde{a}^*) + \left(1 - \frac{2c_x}{\gamma}\right)(1 + \epsilon_2)\,(1 - x) \quad (5.5)$$

for some constants ϵ_1 and ϵ_2, and with $0 < c_x < 1$ and $0 < c_{\tilde{a}}$. For $\hat{x} < x \lessapprox 1$ the linear approximation of P^2 is

$$P^2 : x \mapsto 1 - \gamma\,(c_{\tilde{a}} + (c_{\tilde{a}} - 1)\,\epsilon_1)\,(\tilde{a} - \tilde{a}^*) + (2c_x - 1 + (2c_x - \gamma)\,\epsilon_2)\,(x - 1)\,. \quad (5.6)$$

It follows that the fixed point is asymptotically stable provided that

$$|2c_x - 1 + (2c_x - \gamma)\,\epsilon_2| < 1. \quad (5.7)$$

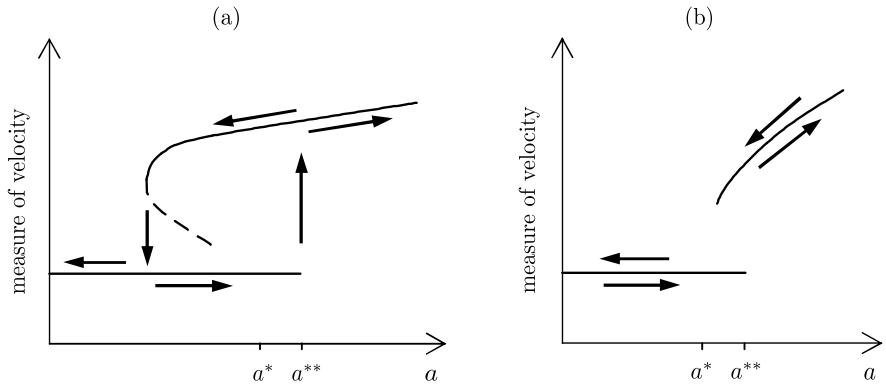

Figure 5.4: Qualitative bifurcation diagram of some measure of the velocity of the impact-oscillator with friction as a function of forcing amplitude when $F_s > F_d$. In panel (a) the parameter values satisfies the opposite inequality of Equation 5.1 and in panel (b) the parameter values satisfies the inequality in Equation 5.1.

The largest-in-magnitude multiplicative error possible while still maintaining stability then occurs for $c_x = 1/2$, in which case

$$|\epsilon_2| < \left| \frac{1}{1-\gamma} \right|. \tag{5.8}$$

For small ϵ_1 and ϵ_2, and with $c_x = 1/2$, x converges to

$$x \approx 1 - \gamma \left(c_{\tilde{a}} + (c_{\tilde{a}} - 1)\, \epsilon_1 + c_{\tilde{a}} \,(1-\gamma)\, \epsilon_2 \right) (\tilde{a} - \tilde{a}^*), \tag{5.9}$$

which yields a residual error of

$$|1 - \gamma c_{\tilde{a}} \,(\tilde{a} - \tilde{a}^*) - x| = \gamma \left| c_{\tilde{a}} + (c_{\tilde{a}} - 1)\, \epsilon_1 + c_{\tilde{a}} \,(1-\gamma)\, \epsilon_2 \right| |\tilde{a} - \tilde{a}^*|. \tag{5.10}$$

To investigate the sensitivity of the proposed control strategies to additive errors in the measurement data, consider the control law

$$\tilde{b}\,(x, \tilde{a}) = \tilde{a}^* - 1 + (1 - c_{\tilde{a}})\,(\tilde{a} - \tilde{a}^* + \delta_1) + \left(1 - \frac{2c_x}{\gamma} \right) (1 - x + \delta_2) \tag{5.11}$$

for some small constants δ_1 and δ_2, and with $0 < c_x < 1$ and $0 < c_{\tilde{a}}$. For $\hat{x} < x \lessapprox 1$ the linear approximation of P^2 is then

$$P^2 : x \mapsto 1 - \gamma c_{\tilde{a}} \,(\tilde{a} - \tilde{a}^*) + (2c_x - 1)\,(x - 1) - \gamma \,(c_{\tilde{a}} - 1)\, \delta_1 + (\gamma - 2c_x)\, \delta_2. \tag{5.12}$$

For example, with $c_x = 1/2$, a residual error

$$|1 - \gamma c_{\tilde{a}} \,(\tilde{a} - \tilde{a}^*) - x| = |\gamma \,(c_{\tilde{a}} - 1)\, \delta_1 + (1 - \gamma)\, \delta_2| \tag{5.13}$$

results.

In summary, using $c_x = 1/2$ is the most robust choice in a control design.

Chapter 6

Discussion and conclusions

This work shows the strength of piecewise-smooth modelling of certain dynamical systems. The hybrid system approach to model impacting systems agrees convincingly with experimental results and the mathematical tools for analysing non-smooth systems are shown to be useful in predicting and drawing conclusions on the dynamic behaviour of such systems. It has also been shown that the framework of hybrid modelling is suitable to construct low-cost control algorithms for the highly nonlinear dynamics of impacting systems.

The major result of **Paper A** is that the transient near-grazing impacting dynamics in a real system, despite the real world noise in parameters and measurements, can be closely approximated by a square-root proportionality from a lowest order expansion of a discontinuity map. In fact, the 'near' in near-grazing dynamics turns out, at least in this particular experiment, not to mean extremely near. The lowest order map actually captures the dynamics for quite considerable impact velocities. Additionally, the map also correctly predicts the number of cycles of the forcing between each impact. As argued in the paper, the presence of a square root makes the growth of impact velocities extremely fast close to grazing which makes a grazing bifurcation a good candidate for construction of a fast limit switch. On the theoretical side, we can note that the somewhat abstract notion of a square-root singularity in the discontinuity map here manifests itself as a concrete square-root growth rate in impact velocity.

Paper B sets the method of a low-cost, discrete, control algorithm for controlling the bifurcation scenario of impact oscillators on a firm theoretical footing. An elegant feature of the proof of stabilizability contained in the paper is that the control algorithm is applicable to impact oscillators with arbitrary degrees of freedom.

The practical application of the proposed low-cost control algorithm in a vehicle suspension, as of **Paper C**, seems to be of limited benefit. The control algorithm works as predicted by the theory, but the benefits compared to a fixed bumpstop is not considerable. In particular, it could not be shown that

the control algorithm could reduce impact velocities while at the same time not increasing the rattle-space of the suspension, a parameter which is already maximized in any given vehicle. The main scientific merits of the paper is instead that the control algorithm is shown to work in piecewise-smooth system with additional discontinuities besides impacts, and that the quarter-car model is presented in a piecewise-smooth framework.

In **Papers D** and **E** the dynamics, and particularly the grazing bifurcation, of an impact oscillator with friction is unfolded in detail, which to the author's knowledge has not been done for this type of system before. It is worth remembering that although the analysis which revealed the bifurcation condition in Equation 5.1 was done locally to the bifurcation point, the condition has impacts on the global dynamics of the system. The inherent instability caused by a loss of a local attractor at a grazing bifurcation, both in the sense of the nature of the ensuing steady-state dynamics as well as the hysteresis effect associated with it, could be a problem in an engineering system. This could be dealt with through the implementation of the low-cost control algorithm derived in **Paper D** for a possible limit-switch or energy-transfer mechanism application.

As a last thought I would like to say that research in dynamical systems (or actually any field of research) should not be based on only a single one of the three basic methods of analysis; numerical simulation, analytical calculations and experiments. At least two, or preferably all three, should be incorporated in any rigorous piece of scientific work. This is a goal I have been striving towards in this work.

Chapter 7

Recommendations for future work

Experimental verification of the bifurcation condition in Equation 5.1 from **Papers D** and **E** would naturally be of interest. Preliminary experimental tests have been conducted with the same equipment as used in the experiments in **Paper A**. However, here the ball-beam assembly was clamped horizontally and with the ball resting on a vertically adjustable surface to introduce dry friction. The idea of the tests is to detect the hysteresis effect as a sign of a non-persistent attractor at the bifurcation point. Some problems with torsional vibration of the leaf spring and insufficient amounts of test runs makes the results inconclusive but there are indications that something significant happens to the interval of hysteresis for some frequency threshold. For example, the overlap in forcing amplitude of impacting and non-impacting solutions was for driving frequencies 6 Hz: 0.100 mm, 5 Hz: 0.149 mm, 4 Hz: 0.024 mm, 3 Hz: 0.005 mm, 2 Hz: 0.028 mm. As can be seen, the overlap is an order of magnitude higher for 5 and 6 Hz compared to 2, 3 and 4 Hz. That the lower frequencies still exhibits a hysteresis effect could be due to the effect of different dynamic and static friction forces as elaborated on in Section 5.3.1. Additional test runs, a solution to the torsional vibration problem and more precise measurements of the parameters of the system is needed for conclusive evidence.

It would also be of interest to map out the dynamics for the parameter ranges not considered in **Papers D** and **E**. Namely, when the frequency ratio $\omega/\omega_0 > 2$ in which case the map of the dynamics close to grazing would be two-dimensional. And also to investigate the dynamics in the case when $a^*\omega^2 < \frac{2F_f}{m(1+e)^2}$, which implies chattering, for $a \approx a^*$. This was only done for $a \leq a^*$ in **Paper D**.

If possible, it would be of interest to derive a general formula for a discontinuity map of grazing impacts in a friction oscillator. The challenge is that in the situation in **Papers D** and **E**, three different vector fields are in play locally

to the grazing point, and the vector field for stick solutions makes solutions in backwards time non-unique.

The realization of the proposed control algorithms of **Papers B**, **C** and **E** in an experimental setup is also of importance. The precision demands on sensors and actuators would be high as the control algorithms rely on minute adjustments of a discontinuity surface.

Paper A proposed the use of the non persistent grazing bifurcation as the triggering event of a mechanical limit switch device. The co-authors of the paper are currently working on further investigations into different designs of such limit switches. Recent results are presented in [67, 68]. This is an example of when a nonlinear effect is explicitly designed for and utilized. Taking advantage of nonlinear effects to construct completely new engineering designs is, and will be, an exciting field of research.

References

[1] Nordin, S., Filosofins historia: det västerländska förnuftets äventyr från Thales till postmodernismen (in Swedish), Studentlitteratur, ISBN 91–44-31851-0, 1995.

[2] Jerrelind, J. and Stensson, A., Nonlinear dynamic behaviour of coupled suspension systems, *Meccanica*, **38**, 43–59, 2003. (doi:10.1023/A:1022067317220)

[3] Dankowicz, H. and Zhao, X., Local analysis of co-dimension-one and co-dimension-two grazing bifurcations in impact microactuators, *Physica D: Nonlinear Phenomena*, **202(3-4)**, pp. 238-57, 2005. (doi:10.1016/j.physd.2005.02.008)

[4] Zhao, X. and Dankowicz, H., Unfolding degenerate grazing dynamics in impact actuators, *Nonlinearity*, **19(2)**, pp. 399-418, 2006. (doi:10.1088/0951-7715/19/2/009)

[5] Zhao, X., Dankowicz, H., Reddy, C.K. and Nayfeh, A.H., Modeling and simulation methodology for impact microactuators, *Journal of Micromechanics and Microengineering*, **14, pp.** 775-784, 2004. (doi:10.1088/0960-1317/14/6/003)

[6] Mason, J.F., Piiroinen, P.T., Wilson, R.E. and Homer, M.E., Basins of attraction in nonsmooth models of gear rattle, *International Journal of Bifurcation and Chaos*, **19(1)**, pp. 203-224, 2009. (doi:10.1142/S021812740902283X)

[7] Lin, Y., Rotor instability induced by radial clearance in ball bearing supports, *ASME: International Gas Turbine and Aeroengine Congress and Exposition*, pp. 1-8, 1993.

[8] Jerrelind, J. and Dankowicz, H., Low-cost control of impact hammer performance, *Proceeding of the 2003 ASME Design Engineering Technical Conferences and Computers and Information in Engineering Conference*, **5**: *19th Biennial Conference on Mechanical Vibration and Noise*, pp. 1547-1554, 2003.

[9] Jerrelind, J. and Dankowicz, H., A global control strategy for efficient control of a Braille impact hammer, *Journal of Vibration and Acoustics, Transactions of the ASME*, **128(2)**, pp. 184-189, 2006. (doi:10.1115/1.2159033)

[10] Stensson, A., Asplund, C. and Karlsson, L., Nonlinear behaviour of a MacPherson strut wheel suspension, *Vehicle System Dynamics*, **23(2)**, pp. 85-106, 1994.

[11] Aidanpää, J.-O., Shen, H.H., Gupta, R.B. and Babic, M., One-dimensional model for the transition from periodic to chaotic motions in granular shear flows, *Mechanics of Materials*, **16(1-2)**: *Mechanics of Granular Materials,* pp. 153-161, 1993.

[12] Jerrelind, J. and Stensson, A., Nonlinear dynamics of parts in engineering systems, *Chaos, Solitons and Fractals*, **11(15)**, pp. 2413-28, 2000. (doi:10.1016/S0960-0779(00)00016-3)

[13] Shaw, S.W. and Holmes, P.J., A periodically forced piecewise linear oscillator, *Journal of Sound and Vibration*, **90**, pp. 129-55, 1983. (doi:10.1016/0022-460X(83)90407-8)

[14] Shaw, S.W., The dynamics of a harmonically excited system having rigid amplitude constraints, Part 1: Subharmonic motions and local bifurcations, *ASME Journal of Applied Mechanics*, **52**, pp. 453-458, 1985.

[15] Shaw, S.W., The dynamics of a harmonically excited system having rigid amplitude constraints, Part 2: Chaotic motions and global bifurcations, *ASME Journal of Applied Mechanics*, **52**, pp.459-464, 1985.

[16] Nordmark, A.B., Non-periodic motion caused by grazing incidence in an impact oscillator, *Journal of Sound and Vibration*, **145(2)**, pp. 279-97, 1991. (doi:10.1016/0022-460X(91)90592-8)

[17] Nordmark, A.B., Effects due to low velocity impact in mechanical oscillators, *International Journal of Bifurcation and Chaos in Applied Sciences and Engineering*, **2(3)**, pp. 597-605, 1992.

[18] Chin, W., Ott, E., Nusse, H.E. and Grebogi, C., Grazing bifurcations in impact oscillators, *Physical Review E*, **50(6),** pp. 4427-44, 1994. (doi:10.1103/PhysRevE.50.4427)

[19] Fredriksson, M.H. and Nordmark, A.B., Bifurcations caused by grazing incidence in many degrees of freedom impact oscillators *Proceedings of the Royal Society A: Mathematical, Physical and Engineering Sciences*, **453(1961)**, pp. 1261-76, 1997.

[20] Fredriksson, M.H., Grazing bifurcations in multibody systems, *Nonlinear Analysis Theory, Methods & Applications*, **30(7)**, pp. 4475-83, 1997. (doi:10.1016/S0362-546X(96)00105-8)

[21] Fredriksson, M.H. and Nordmark, A.B., On normal form calculations in impact oscillators, *Proceedings of the Royal Society A: Mathematical, Physical and Engineering Sciences*, **456(1994)**, pp. 315-29, 2000. (doi:10.1098/rspa.2000.0519)

[22] Fredriksson, M.H., Borglund, D. and Nordmark, A.B., Experiments on the onset of impacting motion using a pipe conveying fluid, *Nonlinear Dynamics*, **19(3)**, pp. 261-71, 1999. (doi:10.1023/A:1008322725617)

[23] Piiroinen, P.T., Virgin, L.N. and Champneys, A.R., Chaos and period-adding: Experimental and numerical verification of the grazing bifurcation, *Journal of Nonlinear Science*, **14(4)**, pp. 383-404, 2004. (doi:10.1007/s00332-004-0616-y)

[24] Stensson, A. and Nordmark, A.B., Experimental investigation of some consequences of low velocity impacts in the chaotic dynamics of a mechanical system, *Philosophical Transactions of the Royal Society A: Mathematical, Physical and Engineering Sciences*, **347(1683)**, pp. 439-48, 1994.

[25] de Weger, J., van de Water, W. and Molenaar, J., Grazing impact oscillations, *Physical Review E (Statistical Physics, Plasmas, Fluids, and Related Interdisciplinary Topics)*, **62(2)**, pp. 2030-41, 2000. (doi:10.1103/PhysRevE.62.2030)

[26] Pavlovskaia, E., Wiercigroch, M. and Grebogi, C., Two-dimensional map for impact oscillator with drift, *Physical Review E*, **70(3 2)**, pp. 036201-1-036201-10, 2004. (doi:10.1103/PhysRevE.70.036201)

[27] Begley, C.J. and Virgin, L.N., Impact response and the influence of friction, *Journal of Sound and Vibration*, **211(5),** pp. 801-818, 1998. (doi:10.1006/jsvi.1997.1389)

[28] Virgin, L.N. and Begley, C.J., Grazing bifurcations and basins of attraction in an impact-friction oscillator, *Physica D*, **130**, pp. 43-57, 1999. (doi:10.1016/S0167-2789(99)00016-0)

[29] Cone, K.M. and Zadoks, R.I., A numerical study of an impact oscillator with the addition of dry friction, *Journal of Sound and Vibration*, **188(5),** pp. 659-683, 1995. (doi:10.1006/jsvi.1995.0617)

[30] Strogatz, S.H., Nonlinear dynamics and chaos, Perseus Books Publishing, LLC: Westview Press, ISBN 0-7382-0453-6, 2000.

[31] di Bernardo, M., Budd, C.J., Champneys, A.R. and Kowalczyk, P., Piecewise-smooth dynamical systems: theory and applications, Springer-Verlag London Limited, ISBN 978-1-84628-039-9, 2008.

[32] The Hybrid Systems Group, http://control.ee.ethz.ch/~hybrid/, August, 2009.

[33] Leine, R., Bifurcations in discontinuous mechanical systems of Filippov type, Doctoral Thesis, Technische Universiteit Eindhoven, ISBN 90-386-2911-7, 2000.

[34] Stronge, W.J., Impact mechanics, Cambridge University Press, ISBN 0-521-63286-2, 2000.

[35] Khalil, H.K., Nonlinear systems, Prentice Hall, ISBN 0-13-1227408, 2000.

[36] Dankowicz, H., Piiroinen, P. and Nordmark, A.B., Low-velocity impacts of quasiperiodic oscillations, *Chaos, Solitons and Fractals*, **14**, pp. 241-255, 2002. (doi:10.1016/S0960-0779(01)00230-2)

[37] Rugh, W.J., Linear systems theory, Second edition, Prentice Hall, ISBN 0-13-441205-2, 1996.

[38] Natsiavas, S., Stability of piecewise linear oscillators with viscous and dry friction damping, *Journal of Sound and Vibration*, **217(3)**, pp. 507-522, 1998. (doi:10.1006/jsvi.1998.1768)

[39] Natsiavas, S., Dynamics of multiple-degree-of-freedom oscillators with colliding components, *Journal of Sound and Vibration*, **165(3),** pp. 439-453, 1993. (doi:10.1006/jsvi.1993.1269)

[40] Verros, G., Natsiavas, S. and Stepan, G., Control and dynamics of quarter-car models with dual-rate damping, *Journal of Vibration and Control*, **6**, pp. 1045-63, 2000. (doi:10.1177/107754630000600706)

[41] Gleick, J., Kaos, vetenskap på nya vägar (original title: Chaos, making a new science), Bonnier Fakta Bokförlag AB, ISBN 91-34-50967-4, 1988.

[42] Moon, F.C., Chaotic and fractal dynamics, John Wiley & Sons, Inc., ISBN 0-471–54571-6, 1992.

[43] Leine, R.I. and Nijmeijer, H., Dynamics and bifurcations of non-smooth mechanical systems, Springer-Verlag Berlin Heidelberg, ISBN 978-3-540-21987-3, 2004.

[44] Dankowicz, H. and Jerrelind, J., Control of near-grazing dynamics in impact oscillators, *Proceedings of the Royal Society A: Mathematical, Physical and Engineering Sciences*, **461(2063)**, pp. 3365-3380, 2005. (doi:10.1098/rspa.2005.1516)

[45] Dormand, J.R. and Prince, P.J., A reconsideration of some embedded Runge-Kutta formulae, *Journal of Computational and Applied Mathematics*, **15(2)**, pp. 203-211, 1986. (doi:10.1016/0377-0427(86)90027-0)

[46] Matlab, The MathWorks, http://www.mathworks.com, August, 2009.

[47] Piiroinen, P.T. and Dankowicz, H., Low-cost control of repetitive gait in passive bipedal walkers, *International Journal of Bifurcation and Chaos*, **15(6)**, pp. 1959-1974, 2005. (doi:10.1142/S0218127405013083)

[48] Wong, J.Y., Theory of ground vehicles, 3rd edition, John Wiley & Sons, Inc., ISBN 0-471-35461-9, 2001.

[49] Verros, G., Natsiavas, S. and Papadimitriou, C., Design optimization of quarter-car models with passive and semi-active suspensions under random road excitation, *Journal of Vibration and Control*, **11**, pp. 581-606, 2005. (doi:10.1177/1077546305052315)

[50] Verros, G. and Natsiavas, S., Dynamics of vehicles with semi-active suspensions exhibiting wheel hop, *Vehicle System Dynamics Supplement*, **35**, pp. 135-148, 2001.

[51] Franklin G.F., Powell J.D. and Emami-Naeini A., Feedback control of dynamic systems, fourth edition, Prentice Hall, ISBN 0-13-032393-4, 2002.

[52] Brogliato, B., On the control of non-smooth complementarity dynamical systems, *Philosophical Transactions of the Royal Society A: Mathematical, Physical and Engineering Sciences*, **359(1789)**, pp. 2369-2383, 2001. (10.1098/rsta.2001.0856)

[53] Gentili, F. and Tornambé, A., Adaptive regulation of impact induced forces for three degree of freedom collisions: A backstepping approach, *Proceedings of the American Control Conference*, pp. 751-755, 1997. (doi:10.1109/ACC.1997.611902)

[54] Chatterjee, S., Non-linear control of friction-induced self-excited vibration, *International Journal of Non-Linear Mechanics*, **42(3)**, pp. 459-69, 2007. (doi:10.1016/j.ijnonlinmec.2007.01.015)

[55] Borrelli, F., Bemporad, A., Fodor, M. and Hrovat, D., An MPC/hybrid system approach to traction control, *IEEE Transactions on control systems technology*, **14(3)**, pp. 541-552, 2006. (doi:10.1109/TCST.2005.860527)

[56] Möbus, R., Baotic, M. and Morari M., Multi-objective adaptive cruise control, *HSCC 2003, LNCS 2623* (eds. O. Maler and A. Pnueli), pp. 359-374, 2003.

[57] Ott, E., Grebogi, C. and Yorke, J.A., Controlling chaos, *Physical Review Letters*, **64(11)**, pp. 1196-1199, 1990. (doi:10.1103/PhysRevLett.64.1196)

[58] Begley, C.J. and Virgin, L.N., On the OGY control of an impact-friction oscillator, *Journal of Vibration and Control*, **7(6)**, pp. 923-931, 2001. (doi:10.1177/107754630100700609)

[59] Faggini, M., Control tools of economic non linear systems, *XIV Riunione Scientifica Siep, Il futuro dei sistemi di welfare nazionali tra integrazione europea e decentramento regionale*, 2002.

[60] Pyragas, K., Continuous control of chaos by self-controlling feedback, *Physics Letters A*, **179,** pp. 421-428, 1992. (doi:10.1016/0375-9601(92)90745-8)

[61] Angulo, F., di Bernardo, M., Fossas, E. and Olivar, G., Feedback control of limit cycles: A switching control strategy based on nonsmooth bifurcation theory, *IEEE Transactions on Circuits and Systems*, **52(2)**, pp. 366-378, 2005. (doi:10.1109/TCSI.2004.841595)

[62] Thota, P. and Dankowicz, H., TC-HAT (TĈ): A novel toolbox for the continuation of periodic trajectories in hybrid dynamical systems, *SIAM Journal on Applied Dynamical Systems*, **7(4)**, pp. 1283-1322, 2008. (doi:10.1137/070703028)

[63] Dankowicz, H. and Schilder, F., An extended continuation problem for bifurcation analysis in the presence of constraints, *Proceedings of the ASME 2009 IDETC/CIE Conference*, 2009.

[64] Dankowicz, H. and Svahn, F., Control of instabilities induced by low-velocity collisions in a vibro-impacting system with friction. In *Vibro-impact dynamics of ocean systems, LNACM* (eds. R. A. Ibrahim, V. I. Babitsky & M. Okuma), **44**, pp. 41–52. Berlin, Heidelberg: Springer-Verlag, 2009. (doi:10.1007/978-3-642-00629-6_5)

[65] Zhao, X. and Dankowicz, H., Control of impact microactuators for precise positioning, *Journal of Computational and Nonlinear Dynamics,* **1(1),** pp. 65-70, 2006. (doi:10.1115/1.1951781)

[66] Dankowicz, H. and Piiroinen, P., Exploiting discontinuities for stabilization of recurrent motions, *Dynamical Systems*, **17(4)**, pp. 317-342, 2002. (doi:10.1080/1468936021000041663)

[67] Wilcox, B., Dankowicz, H. and Lacarbonara, W., Response of electrostatically actuated flexible MEMS structures to the onset of low-velocity contact, *Proceedings of the ASME 2009 IDETC/CIE Conference*, 2009.

[68] Wilcox, B. and Dankowicz, H., Design of limit-switch sensors based on discontinuity-induced nonlinearities, *Proceedings of the ASME 2009 IDETC/CIE Conference*, 2009.

Nomenclature

Typeface

- *Italics* are used when new terms are introduced.
- Mathematical properties are written *slanted*.
- Scalar valued quantities are denoted lower cased and normal faced, such as h. The only exception is P which denotes a scalar valued map.
- Vector valued quantities are denoted lower cased and **bold** faced, such as $\mathbf{x}$.
- Matrices are denoted UPPER cased and **bold** faced, such as $\mathbf{P}$.
- $\mathcal{CALLIGRAPHIC}$ style is used to denote hypersurfaces in state space, such as $\mathcal{P}$.

Notation[1]

a	Amplitude [m]
b	Reference distance between oscillating constraint and mass [m]
b, r, σ	Parameters in the Lorenz equation
$\mathcal{C}$	A Poincaré surface with an associated control map
$\mathbf{c}$	A row vector of control parameters
c_0	A scalar control parameter
d	Damping coefficient [Ns/m]
e	Coefficient of restitution [1]
F	Friction force [N]
$f(t)$	Forcing function [m]
$\mathbf{f}$	Vector field
$\mathbf{g}$	Impact map
$\mathbf{Id}$	The identity matrix, ones on the diagonal and zeros elsewhere
h	Event function
k	Spring stiffness [N/m] or an integer number
m	Mass [kg]
n	An integer number
$\mathcal{O}$	"Big O", $\mathcal{O}(\epsilon^n)$ means of the same size as ϵ^n as $\epsilon \to 0$
$\mathbf{P}$,P	A (Poincaré) map
$\mathcal{P}$	Poincaré surface
$\mathcal{R}$	A subset of state space of the friction oscillator
q	Position [m]
$\mathbb{R}^n$	The set of all n-dimensional column vectors $\mathbf{x}$.
t	Time [s,1]
T	Period: amount of time to complete one oscillatory cycle [s,1]
U	A set in state space enclosing a periodic orbit
$\mathbf{u}$	Column vector of control inputs
v_{rel}	Relative velocity of two bodies [m/s]
$\mathbf{x}$	Column vector containing the states of a system
x	A position, or a state of a system
y, z	States in the Lorenz equation
α	The free parameter in Filippov's method, $\alpha \in [0, 1]$
$\boldsymbol{\beta}$	Vector in the leading order term of the discontinuity map
δ	Position of impact surface, or a small positive number
ϵ	Small positive number
θ	Phase angle [rad]
τ	Time [s,1]
$\mathbf{\Phi}$	The flow, or the collection of all solutions, of a dynamic system
ω	Angular velocity [rad/s]

[1] Units shown where applicable. [s,1] means that the quantity can have the unit of seconds, or have no unit (be non-dimensionalized).

- Sub- and superscripts in conjunction with scalar or vector valued quantities, such as $h_{\mathcal{P}}$ or $\mathbf{x}^*$, are used to distinguish different scalars or vectors.
- A subscript $(\,,)$ denotes differentiation with respect to the variable following it, i.e. $\mathbf{\Phi}_{,t}$ denotes the column vector containing the time derivatives of each component of the flow.
- All vector valued quantities, such as $\mathbf{x}$ and $\mathbf{P}$, are column vectors besides the control vector $\mathbf{c}$ which is a row vector.
- Differentiation of a scalar quantity with respect to a vector, such as $h_{\mathcal{P},\mathbf{x}}(\mathbf{x}^*)$, yields a row vector.
- Matrix products are denoted with a centred dot as in $\mathbf{f}(\mathbf{x}^*) \cdot h_{\mathcal{P},\mathbf{x}}(\mathbf{x}^*)$.